FULL PAPER

Dalton
www.rsc.org/dalton

The synthesis and late transition metal chemistry of 7-aza-*N*-indolyl phosphines and the activity of their palladium complexes in CO–ethene co-polymerisation

Andrew D. Burrows,* Mary F. Mahon and Maurizio Varrone
Department of Chemistry, University of Bath, Claverton Down, Bath, UK BA2 7AY.
E-mail: a.d.burrows@bath.ac.uk

Received 15th August 2003, Accepted 8th October 2003
First published as an Advance Article on the web 23rd October 2003

The 7-aza-*N*-indolyl phosphine ligands $PR_2(N_2C_7H_5)$ (**L**^{1}, R = Ph; **L**^{2}, R = NC_4H_4) were prepared in a two-step process involving treatment of 7-azaindole with BuLi, followed by reaction of the lithium salt with $PClR_2$. **L**^{1} and **L**^{2} react with $[MCl_2(cod)]$ (M = Pd, Pt) to give $[PdCl_2(L\text{-}\kappa^2\textit{P,N})]$ (**1a**, L = **L**^{1}; **1b**, L = **L**^{2}) or $[PtCl_2(L\text{-}\kappa^2\textit{P,N})]$ (**2a**, L = **L**^{1}; **2b**, L = **L**^{2}) and with $[Rh(\mu\text{-}Cl)(cod)]_2$ in the presence of CO to give $[RhCl(CO)(L\text{-}\kappa^2\textit{P,N})]$ (**3a**, L = **L**^{1}; **3b**, L = **L**^{2}). Crystal structures for **1a**,**b** and **3a**,**b** are reported, and structural and spectroscopic evidence confirm that **L**^{2} is a poorer σ-donor/better π-acceptor than **L**^{1}. The complexes $[PdClMe(L\text{-}\kappa^2\textit{P,N})]$ (**4a**, L = **L**^{1}; **4b**, L = **L**^{2}), prepared from [PdClMe(cod)], react with AgOTf to yield $[PdMe(OTf)(L\text{-}\kappa^2\textit{P,N})]$ (**5a**, L = **L**^{1}; **5b**, L = **L**^{2}). Complexes **5a**,**b** are active catalysts for the co-polymerisation of CO and ethene, with activities similar to previously reported catalysts containing *P,N*-donor ligands. From the stepwise insertion reactions of CO and ethene with **5a**,**b**, the acyl complexes $[Pd\{C(O)Me\}(OTf)(L\text{-}\kappa^2\textit{P,N})]$ (**7a**, L = **L**^{1}; **7b**, L = **L**^{2}) and alkyl complexes $[Pd\{CH_2CH_2C(O)Me\text{-}\kappa^2\textit{C,O}\}(L\text{-}\kappa^2\textit{P,N})]OTf$ (**8a**, L = **L**^{1}; **8b**, L = **L**^{2}) have been isolated and crystallographically characterised, and the acyl complexes $[Pd\{C(O)CH_2CH_2C(O)Me\text{-}\kappa^2\textit{C,O}\}(L\text{-}\kappa^2\textit{P,N})]OTf$ (**9a**, L = **L**^{1}; **9b**, L = **L**^{2}) have been spectroscopically characterised. Reactions of **7a** and **9a** with MeOH gave methyl acetate and methyl 4-ketopentanoate respectively, with formation of palladium metal and conversion of the remaining palladium to $[Pd(\mathbf{L}^1\text{-}\kappa^2\textit{P,N})_2](OTf)_2$ **10** which has been crystallographically characterised.

Introduction

Mixed-donor ligands, containing a combination of hard and soft donor sites, have a number of important applications in both coordination chemistry and catalysis including use in cross-couplings,[1] ethene oligomerisations[2] and Heck-type reactions.[3] Recently, we have become interested in *N*-pyrrolyl phosphine ligands in which the presence of one or more P–N bonds to pyrrole rings serves to make the phosphine a strong π-acceptor.[4] Addition of a hard donor atom to such a ligand provides a means of exaggerating the electronic difference between the donor atoms, and we have previously reported the synthesis and chemistry of the keto-functionalised *N*-pyrrolyl phosphines $PPh_2\{NC_4H_3C(O)Me\text{-}2\}$[5] and $P(NC_4H_4)_2\{NC_4H_3C(O)Me\text{-}2\}$.[6] As anticipated, the ligands were observed to become more electron-withdrawing with the increasing number of pyrrolyl substituents.

N-Pyrrolyl phosphine ligands containing nitrogen functionalities have received only limited attention. Ligands containing amine and imine groups have been described and used in rhodium-catalysed hydrosilylation reactions[7] and nickel-catalysed cross-coupling reactions,[8] and recently oxazoline-[9] and cyano-functionalised[10] *N*-pyrrolyl phosphines have been reported. In this paper the syntheses of the *P,N*-donor ligands 7-aza-*N*-indolyldiphenylphosphine **L**^{1} and 7-aza-*N*-indolyldi-*N*-pyrrolylphosphine **L**^{2} are presented, along with the reactions of these ligands with palladium(II), platinum(II) and rhodium(I) centres. In order to evaluate the effects of the anticipated electronic difference between these ligands, preliminary studies on CO–ethene co-polymerisation catalysed by the methyl palladium complexes of **L**^{1} and **L**^{2} are also reported. Since phenyl and *N*-pyrrolyl groups are isosteric,[11] any difference in the structure or reactivity of transition metal complexes containing **L**^{1} and **L**^{2} can be attributed to the difference in the electronic character of the phosphorus donors.

Synthesis of the 7-aza-*N*-indolyl phosphines L^1 and L^2

The ligands **L**^{1} and **L**^{2} were synthesised in a two-step process involving conversion of 7-azaindole to the lithium 7-azaindolyl salt on treatment with BuLi, followed by reaction of this intermediate with either $PClPh_2$ or $PCl(NC_4H_4)_2$. These reactions are shown in Scheme 1, together with the numbering scheme used for the 7-azaindolyl group. It is also possible to synthesise **L**^{1} and **L**^{2} using the reaction between $PClR_2$ and 7-azaindole in the presence of a base such as NEt_3 or DBU (1,8-diazabicyclo[5.4.0]undec-7-ene). However, this proved to be a poor preparative route due to difficulties in separating the desired ligand from by-products and unreacted starting materials.

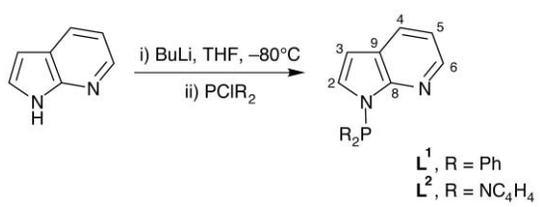

Scheme 1

The $^{31}P\{^1H\}$ NMR spectra of **L**^{1} and **L**^{2} consisted of singlets, at δ 33.4 and δ 72.2 respectively. The observed downfield shift of **L**^{2} with respect to **L**^{1} is consistent with the greater electron withdrawing character of *N*-pyrrolyl substituents compared to phenyl substituents which leads to increased deshielding of the phosphorus nucleus. The ^{1}H NMR spectra were assigned on the basis of ^1H–^1H and ^1H–^{31}P correlation experiments. In the spectrum of **L**^{1} the signal for H_4 was observed as a doublet of unresolved multiplets due to the presence of a small $^5J_{HP}$ coupling in addition to $^3J_{HH}$ and $^4J_{HH}$ coupling. This $^5J_{HP}$ coupling was present in all the 7-aza-*N*-indolyl phosphorus derivatives studied (*vide infra*) and small J_{HP} couplings were also observed in the signals of H_2 and H_3.

The ^{1}H NMR spectrum of **L**^{2} showed distinct resonances for the pyrrolyl ring protons, with the signals for the α and β protons appearing as a *pseudo* quintet and a *pseudo* triplet respectively. The signal for H_4 appeared as a doublet of doublet of doublets due to the coupling with H_5 and H_6 and the

DOI: 10.1039/b309882f

phosphorus atom. The presence of $^5J_{HP}$ was confirmed by the $^1H\{^{31}P\}$ NMR spectrum in which the signal for H_4 collapsed to a doublet of doublets. Signals in the $^{13}C\{^1H\}$ NMR spectra were assigned through ^1H–^{13}C correlation experiments, with quaternary carbons assigned on the basis of their chemical shifts.

Both $\mathbf{L^1}$ and $\mathbf{L^2}$ are air and moisture sensitive and also susceptible to alcoholysis, reacting in methanol to give 7-azaindole and either PPh_2OMe or $P(NC_4H_4)_2OMe$. The observed selective methanolysis of the functionalised pyrrolyl substituent in $\mathbf{L^2}$ is similar to behaviour observed for $P(NC_4H_4)_2\{NC_4H_3C(O)Me\text{-}2\}$,[12] and may simply be a consequence of the functionalised pyrrolyl group being a better leaving group. However, it is also possible that hydrogen bonding between the pyridyl nitrogen atom and the incoming protic nucleophile acts as a directing force, as has been proposed to rationalise the moisture-sensitivity of *N*-pyrazolyl phosphines.[13] Since *N*-indolyl[14] and *N*-carbazolyl[15,16] phosphines have greater tolerance to hydrolysis, the sensitivity of $\mathbf{L^1}$ or $\mathbf{L^2}$ towards protic reagents is unlikely to be related to steric effects.

Palladium(II) and platinum(II) complexes of L^1 and L^2

The reaction of one equivalent of $\mathbf{L^1}$ or $\mathbf{L^2}$ with $[PdCl_2(cod)]$ gave the complexes $[PdCl_2(\mathbf{L^1}\text{-}\kappa^2P,N)]$ **1a** and $[PdCl_2(\mathbf{L^2}\text{-}\kappa^2P,N)]$ **1b** as yellow crystalline materials in good yields. The analogous reactions with $[PtCl_2(cod)]$ led to the complexes $[PtCl_2(\mathbf{L^1}\text{-}\kappa^2P,N)]$ **2a** and $[PtCl_2(\mathbf{L^2}\text{-}\kappa^2P,N)]$ **2b**, as colourless crystalline materials, also in high yield. All four compounds are soluble in chlorinated solvents, and stable in both the solid state and solution. This indicates that coordination of $\mathbf{L^1}$ or $\mathbf{L^2}$ in a chelate manner reduces the instability of the P–N bond, as previously observed with the ketophosphines $PPh_2\{NC_4H_3C(O)Me\text{-}2\}$[5] and $P(NC_4H_4)_2\{NC_4H_3C(O)Me\text{-}2\}$.[6] This is supported by the observation that compounds **1a**,**b** and **2a**,**b** are not susceptible to hydrolysis.

The $^{31}P\{^1H\}$ NMR spectra of **1a**,**b** both consisted of single phosphorus resonances, at δ 80.9 and δ 70.5 respectively, whereas the $^{31}P\{^1H\}$ NMR spectra of **2a**,**b** both comprised singlets, at δ 55.4 and δ 47.3, with ^{195}Pt satellites. The difference in the value of $^1J_{PPt}$ observed for **2b** ($^1J_{PPt}$ 5409 Hz) and **2a** ($^1J_{PPt}$ 4125 Hz) follows the general trend for which an increase in the electronegativity of the substituents on the phosphorus atom causes an increase in the metal–phosphorus coupling constant.[17] In these and other complexes (*vide infra*) the difference in δ between analogous complexes of $\mathbf{L^1}$ and $\mathbf{L^2}$ is much less than in the free ligands, consistent with greater π-backbonding in complexes of $\mathbf{L^2}$ which serves to reduce the deshielding of the phosphorus nucleus.

As for the free ligands, the ^1H NMR spectra of complexes **1a**,**b** and **2a**,**b** were assigned on the basis of ^1H–^1H correlation experiments. Coordination of the pyridyl nitrogen atom to the metal centre causes the signal for H_6 of the 7-azaindolyl ring to be shifted downfield with respect to the free ligands $\mathbf{L^1}$ or $\mathbf{L^2}$ ($\Delta\delta$ 0.70–0.98). A similar downfield shift for the α protons of coordinated pyridine moieties has been reported and used as evidence for coordination of the nitrogen atom.[18] In the ^1H NMR spectra of the platinum complexes **2a**,**b** the signal for H_6 appeared as an unresolved doublet of multiplets with broad ^{195}Pt satellites.

In the ^1H NMR spectrum of **1b**, the signal for H_6 was observed as a doublet of *pseudo* triplets at δ 9.06 with $^4J_{HP}$ through the metal of 1.2 Hz, and the signal for H_4 observed as a doublet of doublet of doublets with $^5J_{HP}$ 1.2 Hz. The presence of these long-range ^1H–^{31}P couplings was confirmed by performing selectively decoupled ^1H NMR experiments. Thus the $^1H\{^{31}P\}$ NMR spectrum of **1b** showed the resonance for H_4 as a doublet of doublets, whilst the ^1H NMR spectrum recorded with the signal for H_6 selectively decoupled also showed this resonance as a doublet of doublets.

Table 1 Selected bond lengths (Å) and angles (°) for complexes **1a**,**b**

1a		**1b**	
Pd(1)–N(2)	2.044(2)	Pd–N(1)	2.0541(13)
Pd(1)–P(1)	2.2144(6)	Pd–P	2.1867(4)
Pd(1)–Cl(1)	2.3444(6)	Pd–Cl(1)	2.3446(4)
Pd(1)–Cl(2)	2.2875(7)	Pd–Cl(2)	2.2899(4)
P(1)–N(1)	1.717(2)	P(1)–N(2)	1.6871(14)
		P(1)–N(3)	1.6681(14)
		P(1)–N(4)	1.6737(14)
N(2)–Pd(1)–P(1)	85.47(6)	N(1)–Pd–P	85.44(4)
N(2)–Pd(1)–Cl(1)	92.22(6)	N(1)–Pd–Cl(1)	93.33(4)
P(1)–Pd(1)–Cl(2)	88.82(2)	P–Pd–Cl(2)	87.341(15)
Cl(2)–Pd(1)–Cl(1)	93.48(2)	Cl(2)–Pd–Cl(1)	93.878(14)
N(2)–Pd(1)–Cl(2)	174.29(6)	N(1)–Pd–Cl(2)	172.78(4)
P(1)–Pd(1)–Cl(1)	177.64(2)	P–Pd–Cl(1)	175.551(14)

The molecular structures of complexes **1a** and **1b** are shown in Figs. 1 and 2 respectively, and selected bond distances and angles are presented in Table 1. The crystal structures confirmed the chelating coordination mode of the ligands, with both complexes showing distorted square planar coordination geometries. The azaindolyl rings are flat, and the ligands

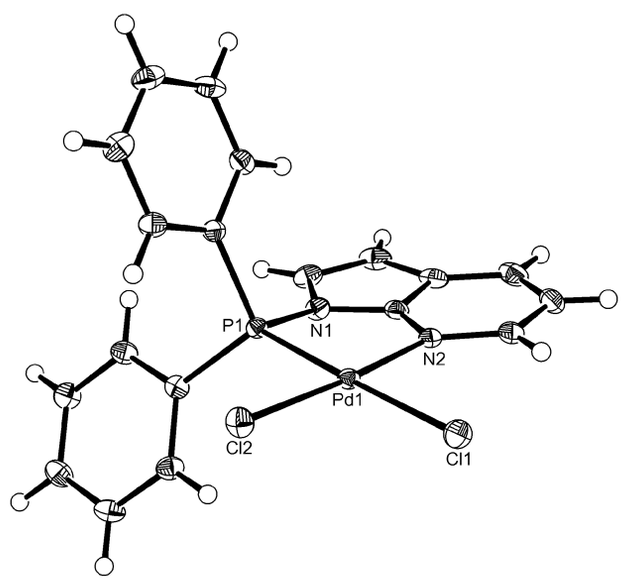

Fig. 1 Molecular structure of $[PdCl_2(\mathbf{L^1})]$ **1a** with the thermal ellipsoids shown at the 30% probability level.

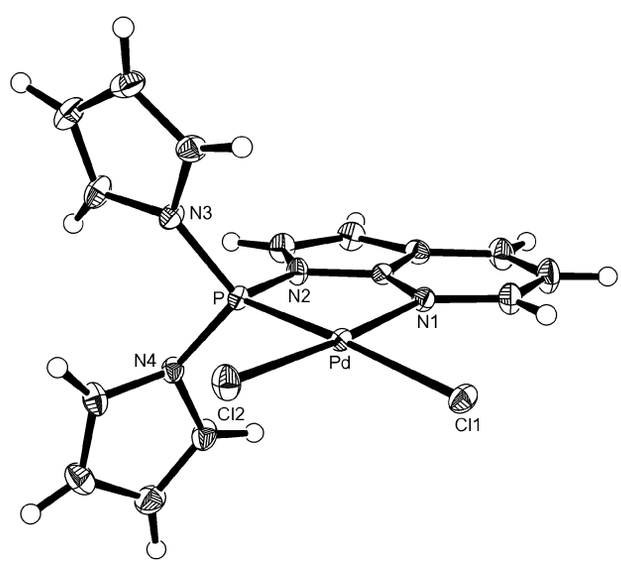

Fig. 2 Molecular structure of $[PdCl_2(\mathbf{L^2})]$ **1b** with the thermal ellipsoids shown at the 30% probability level.

possess crystallographic bite angles of 85.47(6)° for $\mathbf{L^1}$ in **1a** and 85.44(4)° for $\mathbf{L^2}$ in **1b**. These values are larger than those generally observed in phosphine–imine and –amine [19] complexes containing five-membered chelate rings, reflecting the inflexibility of the five-membered chelate rings in complexes of $\mathbf{L^1}$ and $\mathbf{L^2}$.

The Pd–P bond distance in **1b** [2.1867(4) Å] is shorter than that observed in **1a** [2.2144(6) Å], in agreement with the increased double bond character which arises from the greater degree of π-backbonding to $\mathbf{L^2}$. As expected there are no significant differences in the steric requirements of $\mathbf{L^1}$ and $\mathbf{L^2}$ as evidenced by the half crystallographic cone angles of the pyrrolyl (80° and 60°) and phenyl (79° and 61°) groups. The mutually *cis* chlorides have different Pd–Cl bond lengths reflecting the larger *trans* influence of the phosphorus donor over the nitrogen donor. The sums of the angles, $\Sigma\theta$, around the nitrogen atoms in the 7-azaindolyl fragments are similar in **1a**,**b** and within the range 358°–360°, with the exception of N(4) in **1b** for which $\Sigma\theta$ is 352.8°.

Rhodium(I) complexes of $\mathbf{L^1}$ and $\mathbf{L^2}$

The reaction of $[Rh(\mu\text{-}Cl)(cod)]_2$ with two equivalents of either $\mathbf{L^1}$ or $\mathbf{L^2}$ in the presence of CO gave the rhodium(I) carbonyl complexes [RhCl(CO)($\mathbf{L^1}$-κ^2*P,N*)] **3a** and [RhCl(CO)($\mathbf{L^2}$-κ^2*P,N*)] **3b** in good yields. Both complexes were isolated as yellow crystals and fully characterised on the basis of multinuclear NMR and IR spectroscopy, microanalysis and X-ray crystallography. The $^{31}P\{^1H\}$ NMR spectra of **3a**,**b** consisted of doublets with that for **3a** at δ 104.1 ($^1J_{PRh}$ 180 Hz) and that for **3b** at δ 101.9 ($^1J_{PRh}$ 242 Hz). In both cases the resonances are downfield relative to the free ligand, and the greater value of $^1J_{PRh}$ for **3b** is consistent with the anticipated π-acceptor abilities of the phosphorus ligands. These relatively large values of $^1J_{PRh}$ suggest that the complexes both assume coordination arrangements in which the phosphorus atom lies *trans* to the chloride rather than the carbonyl.

The ^1H NMR spectra were as expected, and as with **1a**,**b** and **2a**,**b** the chelating coordination mode of the ligands causes the signals for H_6 of the 7-azaindolyl rings to be shifted downfield with respect to those of the free ligands. The $^{13}C\{^1H\}$ NMR spectra confirmed the geometry suggested by the $^{31}P\{^1H\}$ NMR spectra, with the small values of $^2J_{CP}$ reflecting the mutually *cis* coordination of the carbonyl and phosphorus, as anticipated for the thermodynamically favoured products.[20] The carbonyl stretching frequencies in the IR spectra were observed at 1992 cm^{-1} for **3a** and 2017 cm^{-1} for **3b**. As with the coupling constant information, this provides clear evidence that $\mathbf{L^2}$ has a lower σ-donor/higher π-acceptor ability than $\mathbf{L^1}$.

X-ray structural analyses for complexes **3a** and **3b** confirmed the stereochemistry at the rhodium centres proposed on the basis of the NMR data. The molecular structures are illustrated in Figs. 3 and 4 and selected bond lengths and angles are reported in Table 2. For **3a**, two crystallographically independent molecules were present in the unit cell, though due to their similarity only one molecule is depicted.

The metal centres in **3a**,**b** display distorted square planar geometry with the carbonyl ligand occupying a *trans* position relative to the nitrogen. The crystallographic bite angles for $\mathbf{L^1}$ and $\mathbf{L^2}$, 84.41(8)° and 84.57(7)° for **3a** and 84.27(4)° for **3b**, are very similar to those in the palladium complexes **1a**,**b**. The Rh–P distance is shorter in **3b** [2.1646(4) Å] than in **3a** [2.1977(9) Å and 2.2108(8) Å], and the observed difference in the Rh–P bond distances between **3b** and **3a** is similar to that reported between the complexes *trans*-[RhCl(CO){P(NC$_4$H$_4$)$_3$}$_2$] [Rh–P 2.282(4) Å] and *trans*-[RhCl(CO){PPh$_3$}$_2$] [av. Rh–P 2.325 Å].[4]

The crystallographic half cone angles for the phenyl (av. 70.4°) and pyrrolyl (av. 68.2°) substituents indicate that these are isosteric, and $\Sigma\theta$ around the nitrogen atoms are very close to 360° with the exception of $\Sigma\theta$ around N(3) in **3b** which is 351.9°.

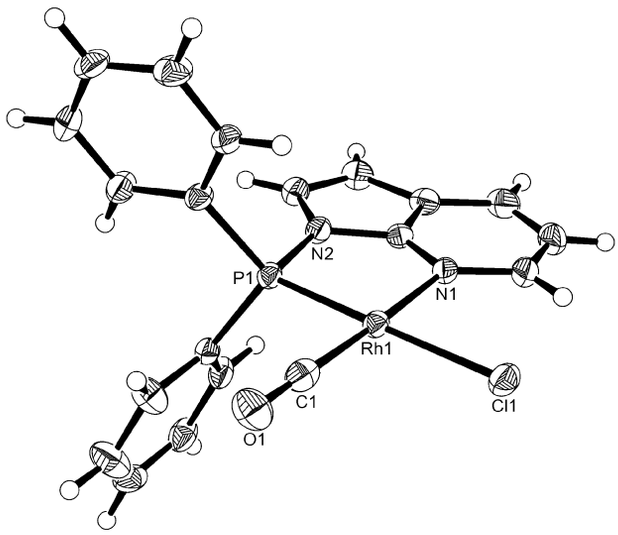

Fig. 3 Molecular structure of [RhCl(CO)($\mathbf{L^1}$)] **3a** with the thermal ellipsoids shown at the 30% probability level.

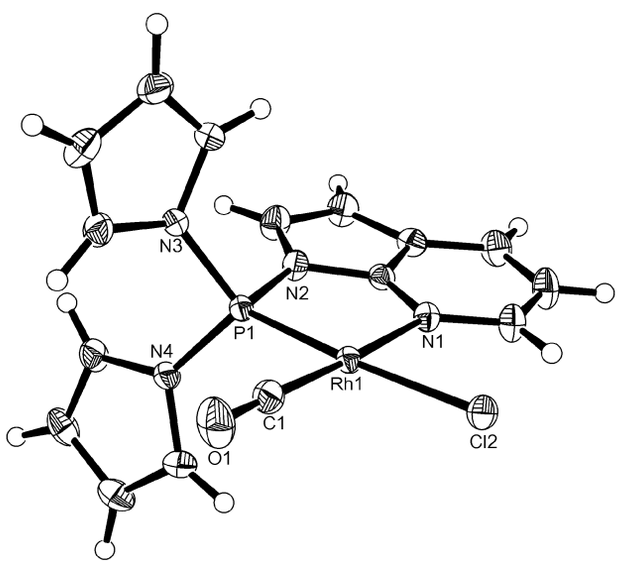

Fig. 4 Molecular structure of [RhCl(CO)($\mathbf{L^2}$)] **3b** with the thermal ellipsoids shown at the 30% probability level.

Synthesis of methylpalladium complexes of $\mathbf{L^1}$ and $\mathbf{L^2}$ and insertion of CO and ethene

The complexes [PdClMe($\mathbf{L^1}$-κ^2*P,N*)] **4a** and [PdClMe($\mathbf{L^2}$-κ^2*P,N*)] **4b** were prepared by the addition of one equivalent of [PdClMe(cod)] to dichloromethane solutions of either $\mathbf{L^1}$ or $\mathbf{L^2}$, and [PdMe(OTf)($\mathbf{L^4}$-κ^2*P,N*)] **5a** and [PdMe(OTf)($\mathbf{L^2}$-κ^2*P,N*)] **5b** were prepared by chloride abstraction with AgOTf from **4a**,**b** respectively. Compounds **4a**,**b** and **5a**,**b** were isolated in almost quantitative yield as air and moisture sensitive crystalline materials and fully characterised. Each of the $^{31}P\{^1H\}$ NMR spectra contained a singlet, shifted significantly downfield relative to the corresponding free ligand. Coordination of the nitrogen atom can be inferred by the chemical shift for the 7-azaindolyl H_6 protons, which are downfield from those of the free ligands, albeit with a smaller displacement than observed for **1a**,**b** and **2a**,**b** ($\Delta\delta$ 0.12–0.37).

The appearance of the resonances for the methyl protons are characteristic of the coordination geometries in these complexes. Those in the ^1H NMR spectra of **4a**,**b** and **5a** appeared as doublets with $^3J_{HP}$ between 1.6 and 4.4 Hz whereas that of **5b** was observed as a singlet. The low magnitude of $^3J_{HP}$ indicates a *cis* arrangement of the phosphorus atom and methyl group and therefore formation of the isomer in which the ligands with

Table 2 Selected bond lengths (Å) and angles (°) for complexes **3a**,**b**

3a (molecule 1)		**3a** (molecule 2)		**3b**	
Rh(1)–C(1)	1.821(4)	Rh(2)–C(21)	1.821(3)	Rh(1)–C(1)	1.8305(19)
Rh(1)–P(1)	2.1977(9)	Rh(2)–P(2)	2.2108(8)	Rh(1)–P(1)	2.1646(4)
Rh(1)–N(1)	2.127(3)	Rh(2)–N(3)	2.109(3)	Rh(1)–N(1)	2.1184(15)
Rh(1)–Cl(1)	2.3752(8)	Rh(2)–Cl(2)	2.3620(8)	Rh(1)–Cl(2)	2.3620(4)
P(1)–N(2)	1.712(3)	P(2)–N(4)	1.722(3)	P(1)–N(2)	1.7006(15)
				P(1)–N(3)	1.6915(15)
				P(1)–N(4)	1.6837(16)
N(1)–Rh(1)–P(1)	84.41(8)	N(3)–Rh(2)–P(2)	84.57(7)	N(1)–Rh(1)–P(1)	84.27(4)
P(1)–Rh(1)–C(1)	90.30(11)	P(2)–Rh(2)–C(21)	93.30(10)	P(1)–Rh(1)–C(1)	92.05(6)
C(1)–Rh(1)–Cl(1)	93.18(11)	C(21)–Rh(2)–Cl(2)	90.93(10)	C(1)–Rh(1)–Cl(2)	91.54(6)
Cl(1)–Rh(1)–N(1)	92.04(8)	Cl(2)–Rh(2)–N(3)	91.28(7)	Cl(2)–Rh(1)–N(1)	92.12(4)
N(1)–Rh(1)–C(1)	173.92(13)	N(3)–Rh(2)–C(21)	177.67(12)	N(1)–Rh(1)–C(1)	176.30(7)
P(1)–Rh(1)–Cl(1)	176.18(3)	P(2)–Rh(2)–Cl(2)	173.06(3)	P(1)–Rh(1)–Cl(2)	175.852(16)

the largest *trans* influence are *cis* to each other. The lower value for $^{3}J_{HP}$ for complexes of $\mathbf{L^2}$ is in agreement with this being a poorer σ-donor than $\mathbf{L^1}$. The signals for the methyl group in the $^{13}C\{^{1}H\}$ NMR spectra appeared as singlets or as doublets with small $^{2}J_{CP}$ confirming this geometry.

The reactions of complexes **4a**,**b** and **5a**,**b** with CO in CD_2Cl_2 at ambient temperature were followed by $^{31}P\{^{1}H\}$ and ^{1}H NMR spectroscopy. The insertion of CO into the Pd methyl bond of **4a**,**b** and **5a**,**b** produced the palladium acyl complexes [PdCl{C(O)Me}($\mathbf{L^1}$-κ^2*P*,*N*)] **6a**, [PdCl{C(O)Me}($\mathbf{L^2}$-κ^2*P*,*N*)] **6b**, [Pd{C(O)Me}(OTf)($\mathbf{L^1}$-κ^2*P*,*N*)] **7a** and [Pd{C(O)Me}(OTf)-($\mathbf{L^2}$-κ^2*P*,*N*)] **7b** respectively. These complexes were isolated as crystalline materials and fully characterised by NMR and IR spectroscopy. In addition the structures of **7a** and **7b** were confirmed crystallographically.

Complexes **6a**,**b** and **7a**,**b** are air and moisture sensitive, decomposing when exposed to moisture to yield palladium metal. This feature prevented satisfactory elemental analyses for **6b** and **7a**,**b** from being obtained. The CO insertion reactions are irreversible, as evidenced by the fact that both the $^{31}P\{^{1}H\}$ and ^{1}H NMR spectra of **6a**,**b** and **7a**,**b** did not undergo any significant changes for more than 24 h on removal of unreacted CO.

The reactions of the chloro methyl complexes **4a**,**b** to produce **6a**,**b** were slow, requiring more than 24 h to reach completion. In contrast **5a**,**b** exhibited reaction times of a few minutes, which parallels previous results showing that the use of more weakly-coordinating anions causes an increase in the rate of CO insertion.[21]

The complexes **6a**,**b** and **7a**,**b** afforded very similar spectroscopic data, suggesting structural similarities. The IR spectra showed strong absorptions in the range 1697–1729 cm^{-1} which are typical for Pd-acyl C=O stretches. In the $^{31}P\{^{1}H\}$ NMR spectra significant upfield shifts characteristic of the insertion of CO in the Pd–Me bond were observed. The ^{1}H NMR spectra showed significant downfield shifts for the resonances of the methyl group and little change in the aromatic region. In the $^{13}C\{^{1}H\}$ NMR spectra the signals for the methyl groups were significantly shifted compared with those of the parent palladium methyl complexes and appeared as doublets with $^{3}J_{CP}$ in the range 29–46 Hz. The resonances for the carbonyl group were observed in the expected range as doublets with small $^{2}J_{CP}$ coupling constants. The magnitude of $^{3}J_{CP}$ and $^{2}J_{CP}$ suggest that the acyl group is *cis* to the phosphorus.

In monitoring the CO insertion reaction by ^{1}H and $^{31}P\{^{1}H\}$ NMR spectroscopy no signals apart from those of the starting materials and the products were observed, indicating that the necessary *pre*- or *post*- insertion isomerisation reactions, one of which must have occurred to give the observed product, are too fast to be detected at ambient temperature.[22]

In an effort to detect the presence of palladium acyl carbonyl complexes such as [Pd{C(O)Me}(CO)($\mathbf{L^1}$-κ^2*P*,*N*)]OTf, a CD_2Cl_2 solution of **5a** was exposed to an atmosphere of ^{13}CO, and $^{31}P\{^{1}H\}$, $^{13}C\{^{1}H\}$ and ^{1}H NMR spectra were recorded both at ambient temperature and −70 °C. The $^{31}P\{^{1}H\}$ NMR spectrum showed the phosphorus resonance for **7a** as a doublet centred at δ 65.5 with $^{2}J_{CP}$ 6 Hz, whereas the $^{13}C\{^{1}H\}$ NMR spectrum showed an intense doublet at δ 220.5 with $^{2}J_{CP}$ 6 Hz, assigned to the acyl group of **7a**. The ^{1}H NMR spectrum showed the protons of the methyl group as a doublet of doublets centred at δ 2.28 with $^{4}J_{HP}$ 1.2 Hz and $^{2}J_{HC}$ 6.0 Hz. These data are consistent with ^{13}C-labelled **7a** and indicate the absence, under these reaction conditions, of significant amounts of any palladium acyl carbonyl complexes.

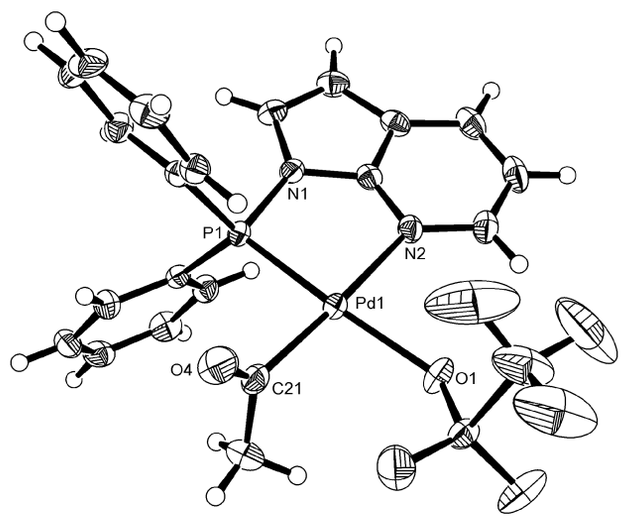

Fig. 5 Molecular structure of [Pd{C(O)Me}(OTf)($\mathbf{L^1}$)] **7a** with the thermal ellipsoids shown at the 30% probability level.

The structures of complexes **7a** and **7b** were confirmed by X-ray crystallography. Crystals suitable for X-ray diffraction studies were obtained by slow diffusion of hexane into CD_2Cl_2 solutions under an atmosphere of CO. The crystal structures of **7a**,**b** are shown in Figs. 5 and 6 with selected bond distances and angles given in Table 3. Complex **7a** crystallised with three independent molecules in the asymmetric unit but for clarity reasons only one of these is depicted in Fig. 5.

The solid state structures are consistent with the solution structures, showing the palladium centres in distorted square planar coordination geometries with the acyl group and the phosphorus atom occupying relative *cis* positions. Deviations from idealised square planar coordination geometries are small as evidenced by the values of the *cis* and *trans* angles at the palladium centres. The Pd–N bond distances are longer in the structures of **7a**,**b** than in those of **1a**,**b**, which reflects the increased *trans* effect of the acyl group compared with chloride. The Pd–C distances in **7a**,**b** are both normal for palladium acyl bonds *trans* to nitrogen atom, and the acyl groups adopt

Table 3 Selected bond lengths (Å) and angles (°) for complexes **7a**,**b**

		7b		
	7a	Molecule 1	Molecule 2	Molecule 3
Pd–P	2.2106(6)	2.1796(12)	2.1851(11)	2.1813(11)
Pd–N	2.193(2)	2.190(4)	2.196(4)	2.205(4)
Pd–O	2.1345(16)	2.151(4)	2.119(4)	2.143(3)
Pd–C	1.994(3)	1.989(5)	1.993(5)	1.990(5)
P–N[a]	1.718(2)	1.694(4)	1.684(4)	1.697(4)
P–Pd–N	85.89(5)	85.39(10)	84.59(10)	84.17(10)
N–Pd–O	88.53(7)	92.02(14)	93.17(14)	97.39(12)
O–Pd–C	95.59(8)	90.60(18)	90.95(17)	86.60(15)
C–Pd–P	89.83(7)	91.96(15)	91.76(13)	91.71(13)
P–Pd–O	173.67(5)	169.50(10)	171.44(11)	175.93(8)
N–Pd–C	174.85(9)	177.35(18)	174.90(17)	175.49(15)

[a] Azaindolyl nitrogen atoms.

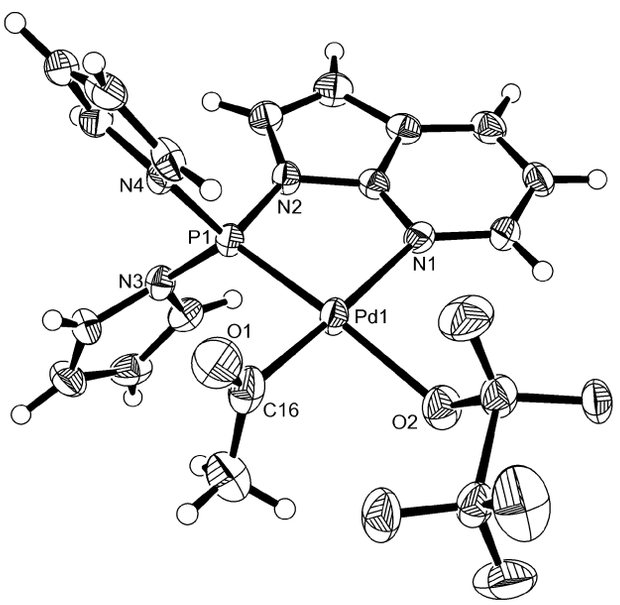

Fig. 6 Molecular structure of [Pd{C(O)Me}(OTf)(**L**^{2})] **7b** with the thermal ellipsoids shown at the 30% probability level.

orientations approximately perpendicular to the metal coordination planes.

As observed in the X-ray crystal structures of **1a**,**b** and **3a**,**b**, substitution of the two phenyl rings with two *N*-pyrrolyl rings leads to a decrease in the M–P bond distance by approximately 0.03 Å. $\Sigma\theta$ around the nitrogen atoms in both structures are close to 360° in agreement with their formal sp^2 hybridisations. However, as observed in the structures of **1b** and **3b**, one of the nitrogen atoms of the pyrrolyl substituents in **7b** has a significant pyramidal distortion (mean 353°).

The insertion of ethene in the palladium acyl bonds of complexes **7a**,**b** produced the alkyl complexes [Pd{CH_2CH_2C(O)Me-κ^2*C*,*O*}(**L**^{1}-κ^2*P*,*N*)]OTf **8a** and [Pd{CH_2CH_2C(O)Me-κ^2*C*,*O*}(**L**^{2}-κ^2*P*,*N*)]OTf **8b**. These reactions were slower than the CO insertions, requiring several hours to reach completion. The conversions of **7a** into **8a** and **7b** into **8b** were monitored by NMR spectroscopy, which indicated that, as for the CO insertion reactions, the *pre*- or *post*- isomerisations necessary to generate the observed isomers are too fast to be detected.

The configurations of **8a**,**b** were determined by multinuclear NMR and IR spectroscopy and confirmed by X-ray single crystal diffraction studies. The ^{31}P{^{1}H} NMR spectra of **8a**,**b** showed singlets, at δ 84.3 and δ 91.1 respectively, which are shifted to low field with respect to **7a**,**b**. In the ^{1}H NMR spectrum of **8a**, the chemically inequivalent methylene groups gave rise to two distinctive signals at δ 3.16 and δ 1.99. The former was assigned to the CH_2 group bonded to the acyl group and appears as a triplet due to the coupling with the other methylene group ($^3J_{HH}$ 6.2 Hz), whereas the latter was assigned to the CH_2 group bonded to the palladium and appears as a triplet of doublets due to an additional coupling with the phosphorus atom ($^3J_{HP}$ 1.2 Hz). The methyl protons were observed as a singlet at δ 2.49. The ^{1}H NMR spectrum of **8b** presented similar features to that of **8a** though the signals for the protons of the methylene groups appeared as distinct but unresolved multiplets.

The ^{13}C{^{1}H} NMR spectra of **8a**,**b** were assigned on the basis of ^{1}H–^{13}C NMR correlation experiments. The only unexpected feature is the presence in both spectra of a $^4J_{CP}$ coupling of 3 Hz between the phosphorus atom and the carbon of the methyl group. The IR spectra showed strong ν(CO) absorptions at 1631 cm^{-1} for **8a** and 1628 cm^{-1} for **8b**, which are shifted to lower frequency relative to those for the parent acyl complexes (**7a**, 1711 cm^{-1}; **7b** 1729 cm^{-1}) indicating coordination of the ketonic oxygen.

Crystals of **8a** and **8b** suitable for X-ray crystallographic studies were obtained by the slow diffusion of hexane into CD_2Cl_2 solutions saturated with ethene. The structures of **8a** and **8b** are shown in Figs. 7 and 8 while selected bond distances and angles are given in Table 4. The metal centre in both complexes exhibits a distorted square planar coordination geometry with the coordinated ketonic oxygen *trans* to the phosphorus. The most significant difference between the structures is the Pd–P bond length, which is longer in **8a** than in **8b** by 0.03 Å, in a similar manner to the other structures in this paper (*vide supra*).

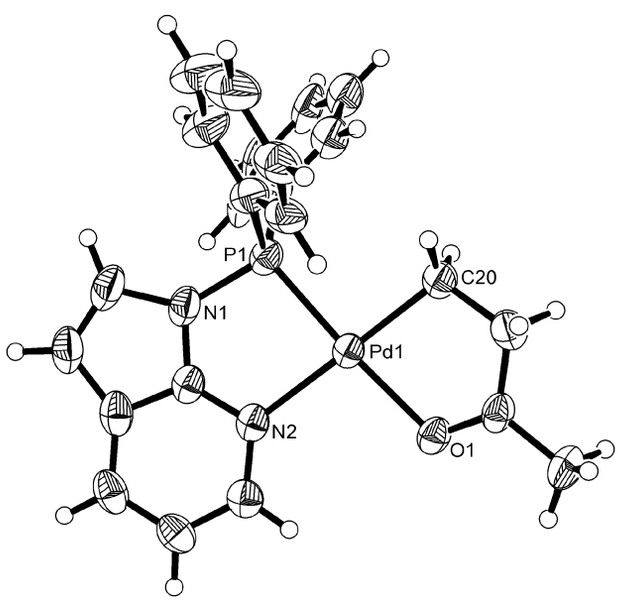

Fig. 7 Molecular structure of [Pd{CH_2CH_2C(O)Me-κ^2*C*,*O*}(**L**^{1})]OTf **8a** with the thermal ellipsoids shown at the 30% probability level and the anion omitted for clarity.

8a and **8b** were further reacted with CO to yield [Pd{C(O)CH_2CH_2C(O)Me-κ^2*C*,*O*}(**L**^{1}-κ^2*P*,*N*)]OTf **9a** and [Pd{C(O)CH_2CH_2C(O)Me-κ^2*C*,*O*}(**L**^{2}-κ^2*P*,*N*)]OTf **9b**. Both reactions were monitored by NMR spectroscopy and found to be considerably slower than the CO insertion reactions into **5a**,**b**, requiring several hours to reach completion. This decrease in reactivity has been observed before for similar palladium complexes and rationalised on the basis of the 5-membered metallocyclic ring needing to open for CO to coordinate.[23] However, it is notable that analogous complexes to **8a**,**b** containing phosphine–imine ligands do not react with CO in dichloromethane, requiring the presence of acetonitrile to facilitate reaction.[24] In contrast to the reactions of **5a**,**b** with CO, the reactions of **8a**,**b** with CO are reversible. Consequently **9a**,**b** were only observed in solutions saturated with CO.

Table 4 Selected bond lengths (Å) and angles (°) for complexes **8a**,**b**

8a		**8b**	
Pd(1)–C(20)	2.029(4)	Pd(1)–C(1)	2.027(5)
Pd(1)–O(1)	2.102(2)	Pd(1)–O(1)	2.102(3)
Pd(1)–N(2)	2.137(3)	Pd(1)–N(1)	2.148(4)
Pd(1)–P(1)	2.1808(10)	Pd(1)–P(1)	2.1532(15)
C(22)–O(1)	1.238(4)	C(3)–O(1)	1.250(6)
P(1)–N(1)	1.716(3)	P(1)–N(2)	1.692(4)
		P(1)–N(3)	1.694(4)
		P(1)–N(4)	1.666(4)
N(2)–Pd(1)–P(1)	85.69(9)	N(1)–Pd(1)–P(1)	85.31(12)
C(20)–Pd(1)–O(1)	82.88(13)	C(1)–Pd(1)–O(1)	83.57(19)
O(1)–Pd(1)–N(2)	97.98(11)	O(1)–Pd(1)–N(1)	97.80(16)
C(20)–Pd(1)–P(1)	93.46(11)	C(1)–Pd(1)–P(1)	93.33(16)
O(1)–Pd(1)–P(1)	175.92(7)	O(1)–Pd(1)–P(1)	174.43(10)
C(20)–Pd(1)–N(2)	179.11(13)	C(1)–Pd(1)–N(1)	178.6(2)

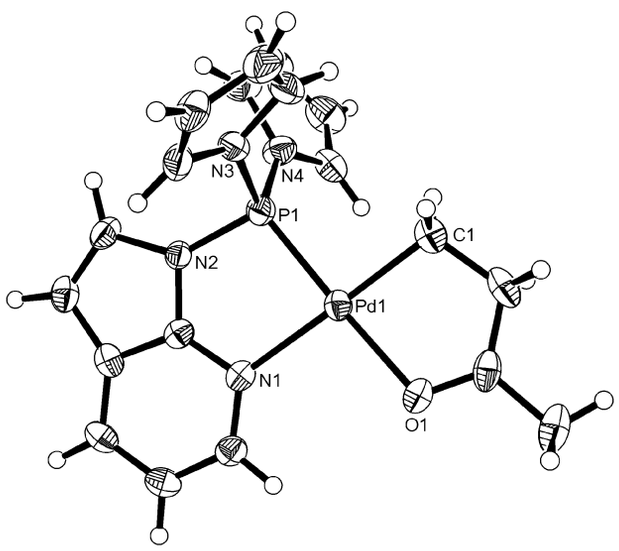

Fig. 8 Molecular structure of [Pd{$CH_2CH_2C(O)Me$-κ²*C,O*}(**L²**)]OTf **8b** with the thermal ellipsoids shown at the 30% probability level and the anion omitted for clarity.

The $^{31}P\{^1H\}$ NMR spectra of **9a**,**b** both consisted of singlets, shifted to high field with respect to **8a**,**b**. The ^1H NMR spectra showed the signal for the 7-azaindolyl H_6 proton at δ 8.42 as a broad doublet for **9a** and at δ 8.45 as a doublet of doublets for **9b**. In both cases the methylene protons were observed as a multiplet between δ 2.7 and δ 2.9. The only signals observed in the NMR spectra were those assigned to the products and starting materials, so as for the insertions of CO into **5a**,**b** and ethene into **7a**,**b**, the *pre* or *post* isomerisation processes are too fast to be detected.[22] The IR spectra showed two distinctive carbonyl stretching frequencies (**9a**, 1711, 1622 cm^{-1}; **9b** 1716, 1660 cm^{-1}) consistent with the presence of coordinated and uncoordinated carbonyl groups.

Following the studies on the stepwise migratory insertion reactions, CO and ethene were bubbled simultaneously into a CD_2Cl_2 solution of **5a** and the reaction monitored by NMR spectroscopy. The spectra showed that CO and ethene insertion reactions progress consecutively. Within a few minutes **5a** is converted into **7a**, which over the course of 2 h reacts with ethene to produce **8a**. Continued passage of CO and ethene through the solution did not result in the formation of **9a** which evidently requires higher CO pressure and/or longer reaction times to be formed.

In order to determine the relative rates of insertion for the complexes of **L¹** and **L²**, equimolar amounts of **5a**,**b** were dissolved in CD_2Cl_2, exposed to an atmosphere of CO and ethene and the reactions monitored by NMR spectroscopy. Since it was of interest to record spectra that contain the signals for both starting materials and products, the applied pressures of both monomers were kept low. Before exposure to ethene, excess CO was removed by freezing the sample with liquid nitrogen and applying a reduced pressure. Conversions were determined by comparing the integrals in the $^{31}P\{^1H\}$ and ^1H NMR spectra for the insertion products with those of the parent compounds. The results indicated that the insertion of CO into the palladium methyl bond of **5b** is approximately 1.3 times faster than in that of **5a**, whereas ethene insertion into the palladium acyl bond in **7a** is approximately 3 times faster than in **7b**. Although the former finding is not likely to be significant, the latter result is consistent with the greater stability of the Pd–O bond *trans* to the more electron withdrawing **L²** thus reducing the rate of anion loss in **7b** over **7a**.

Catalytic CO ethene co-polymerisation experiments

Following on from the insertion studies, a series of catalytic test reactions for the CO–ethene co-polymerisation[23,25] catalysed by **5a**,**b** was undertaken. While this reaction is normally carried out with *P,P*-[26] or *N,N*-[27] donor ligands, there have been a number of reports on the activity of complexes containing *P,N*-donor ligands in this reaction.[19,24,28] Although less active than catalysts with homotopic ligands, use of these heterotopic ligands has allowed a number of key intermediates to be isolated and crystallographically characterised. The activities (Table 5) are expressed in grams of polyketone (PK) per gram of palladium based on the mass of the insoluble material isolated at the end of each run. Pure white precipitates were obtained only in the experiments performed in pure dichloromethane (runs 1 and 4). All the other experiments produced off-white materials owing to the presence of some palladium metal. Analysis of the filtrate from runs 2, 3 and 5 by ^1H NMR spectroscopy did not reveal detectable quantities of methylpropanoate—the product of the hydromethoxycarbonylation of ethene. Catalytic reactions performed in pure methanol did not produce any PK or methylpropanoate and led only to the decomposition of the catalysts.

Characterisation of the obtained polymeric materials was performed by $^{13}C\{^1H\}$ NMR and IR spectroscopy and by measurement of the melting points. The IR spectra of the polymeric materials isolated from all the runs were very similar and contained an intense carbonyl absorption band at 1695 cm^{-1} in agreement with previous results.[23] The melting points were observed at temperatures around 250 °C and are in the range reported in the literature (240–260 °C) for polymers with a CO content of 50%, alternating structures and high molecular weights.[29] The $^{13}C\{^1H\}$ NMR spectra contained resonances at δ 213.1 and δ 36.1 with intensities in the ratio 1:2, which can be assigned to the methylene and carbonyl carbons of PK respectively.

Low intensity signals were observed in the range δ 0–50, assignable to the terminal groups of the polymeric chain. The intensity ratios indicated a molecular mass of approximately 23000.[30] $^{13}C\{^1H\}$ NMR spectra for PK isolated from the reactions in the presence of methanol showed an increase in intensity of the signals from the end groups, implying a decrease in the molecular weights of the obtained polymers.

These reactions demonstrate that **5a**,**b** are active catalysts for the CO–ethene co-polymerisation, with **5b** affording a slightly higher activity than **5a**. The polymeric materials isolated from the reaction catalysed by both complexes have similar molecular weights. The obtained activities for **5a**,**b** are comparable with those reported for palladium catalysts modified with other heteroditopic bidentate ligands, though low if compared with the activities obtained using palladium complexes modified with diphosphine ligands.[19,24,28] An increase in the pressure of the monomers as well as the presence of an acid co-catalyst (run 6) resulted in an increase in the quantity of the isolated polymers.

Table 5 Catalytic results for complexes **5a**,**b** in the co-polymerisation of CO and ethene[a]

Run	Complex	*n*/mmol	*p*(CO)/psi	$p(C_2H_4)$/psi	*T*/°C	*t*/h	MeOH	PK/mg	g(PK)/g(Pd)
1	**5a**	0.017	20	20	50	24	0	70	38
2	**5a**	0.061	30	30	25	24	300 µl	150	22
3	**5a**	0.075	40	40	25	48	10 ml	330	82
4	**5b**	0.047	20	20	50	20	0	320	64
5	**5b**	0.042	20	20	25	24	500 µl	240	55
6	**5b**[b]	0.045	20	20	50	20	0	700	146

[a] Solvent CH_2Cl_2 (50 ml). [b] 5 µl of HSO_3CF_3 added.

Methanol-induced termination reactions

The catalytic experiments demonstrated that methanol has a negative effect in the co-polymerisation of CO and ethene catalysed by **5a**,**b**. However as the molecular weight of the polymers obtained from the experiments performed with small amounts of methanol remained quite high, the decrease in activity could be due to the lack of an efficient chain transfer process with the termination reactions not producing species able to start a new catalytic cycle. This may also explain why methylpropanoate is not produced in the catalytic experiments performed in the presence of methanol and why the catalytic reactions in pure methanol ended with complete catalyst decomposition.

According to the proposed mechanism for the CO–ethene co-polymerisation in methanol,[23] two termination reactions are possible: protonolysis of the palladium alkyl bond of complexes similar to [Pd{$CH_2CH_2C(O)Me$-κ^2C,O}($\mathbf{L^1}$-κ^2P,N)]OTf **8a** or methanolysis of a palladium acyl bond of complexes similar to [Pd{C(O)Me}(OTf)($\mathbf{L^1}$-κ^2P,N)] **7a** and [Pd{$C(O)CH_2CH_2C(O)Me$-κ^2C,O}($\mathbf{L^1}$-κ^2P,N)]OTf **9a**. In order to establish which of the two termination processes is active in the CO–ethene co-polymerisation experiments catalysed by complexes **5a**,**b**, the reactions of **7a**, **8a** and **9a** with approximately equivalent amounts of methanol in CD_2Cl_2 at ambient temperature were followed by multinuclear NMR spectroscopy. The ^{1}H NMR spectra for the reactions of **7a** and **9a** showed that methanol is quantitatively converted to methyl acetate and methyl 4-keto-pentanoate respectively. Both reactions were slow, taking more than 24 h to reach completion, and proceeded with the precipitation of significant amounts of palladium black. On the contrary, the ^{1}H and ^{31}P{^{1}H} NMR spectra for **8a** showed no significant variation after 2 days. In the ^{31}P{^{1}H} NMR spectra for the reactions of **7a** and **9a** with MeOH, the disappearance of the signals for the starting material is accompanied by the appearance of a new singlet resonance at δ 90.2 thus indicating that both complexes are converted quantitatively into a new palladium complex **10**. The ^{1}H NMR spectra for **10** showed complex signals in the aromatic region, which were difficult to interpret, but no signal in the alkyl region.

Filtration of the solution to remove palladium, followed by layering with hexane gave crystalline material suitable for X-ray crystallography, which subsequently revealed the identity of **10** to be the dicationic palladium complex *cis*-[Pd($\mathbf{L^1}$-κ^2P,N)$_2$](OTf)$_2$. The molecular structure of **10**·1.5H_2O is shown in Fig. 9 and selected bond lengths and angles are reported in Table 6. The palladium centre has a distorted square planar coordination geometry with the $\mathbf{L^1}$ ligands coordinated in a *cis* orientatation. The Pd–N bond distances of 2.115(3) Å and 2.127(4) Å are appreciably longer than the Pd–N bond distance in **1a**, indicating the higher *trans* influence of the diphenylphosphino group compared to chloride in addition to steric effects. The two planes of the 7-aza-indolyl rings are not coplanar but twisted by approximately 22°, which is probably a consequence of the steric repulsion between the H_6 hydrogen atoms on the azaindolyl rings. A separation between the two hydrogen atoms of 2.15 Å is observed, whereas in a hypothetical planar structure this distance would have been 1.5 Å.

Table 6 Selected bond lengths (Å) and angles (°) for complex **10**

Pd(1)–P(1)	2.2602(11)
Pd(1)–P(2)	2.2481(12)
Pd(1)–N(2)	2.127(4)
Pd(1)–N(4)	2.115(3)
P(1)–N(1)	1.705(4)
P(2)–N(3)	1.705(4)
N(4)–Pd(1)–N(2)	97.73(14)
N(2)–Pd(1)–P(1)	83.85(10)
N(4)–Pd(1)–P(2)	84.56(11)
P(2)–Pd(1)–P(1)	94.50(4)
N(2)–Pd(1)–P(2)	172.32(11)
N(4)–Pd(1)–P(1)	174.87(10)

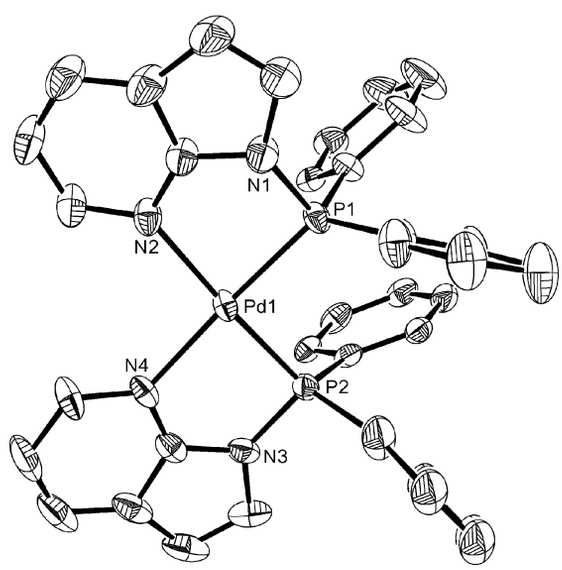

Fig. 9 Molecular structure of [Pd($\mathbf{L^1}$)$_2$](OTf)$_2$ **10** with the thermal ellipsoids shown at the 30% probability level and the anions omitted for clarity.

In order to confirm that *cis*-[Pd($\mathbf{L^1}$)$_2$](OTf)$_2$ is the compound observed in solution, this and the analogous platinum complex *cis*-[Pt($\mathbf{L^1}$-κ^2P,N)$_2$](OTf)$_2$ **11** were synthesised in a more logical manner. Thus the reaction of [$PdCl_2$(cod)] with two equivalents of $\mathbf{L^1}$ in the presence of AgOTf gave **10** whereas the reaction of **2a** with one equivalent of $\mathbf{L^1}$ in the presence of AgOTf gave **11**. The product from the [$PdCl_2$(cod)] reaction exhibited identical spectra to **10**, whereas the ^{31}P{^{1}H} NMR spectrum of **11** consisted of a singlet at δ 62.8 with ^{195}Pt satellites ($^1J_{PPt}$ 3601 Hz). The high value of $^1J_{PPt}$ is indicative of a *cis* arrangement of the two phosphorus atoms in a similar manner to that observed in **10**.

The methanolysis of **7b** proceeded in an analogous manner to that of complex **7a**, converting methanol into methyl acetate on the basis of ^{1}H NMR spectroscopy. The ^{31}P{^{1}H} NMR spectra showed the progressive disappearance of the signal

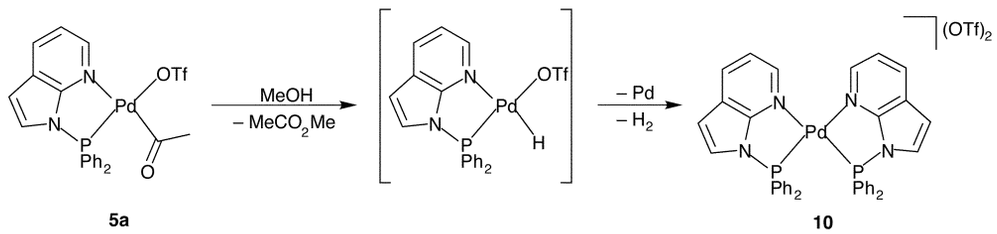

5a **10**

Scheme 2

assigned to **7b** and appearance of a broad singlet at δ 129.6 which was tentatively assigned to $[Pd(\mathbf{L}^2)_2](OTf)_2$, though attempts to isolate this complex were unsuccessful.

Since the reaction of **7a** with methanol proceeded with the conversion of methanol into methyl acetate, this suggests the initial step in the conversion of **7a** to **10** involves formation of a palladium hydride complex. ^{1}H NMR spectra of the crude reaction mixture contained signals in the hydride region though unfortunately this intermediate could not be fully characterised or isolated because of its ready decomposition into **10** and palladium black. This finding begged the question of whether or not **10** itself was active in the CO–ethene co-polymerisation; however the failure of **10** to react with CO or ethene either in the presence or absence of methanol indicated that this is not so.

The formation of palladium hydride complexes through methanolysis of palladium acyl complexes has been reported previously.[31] In particular the reaction of methanol with [PdCl{C(O)Me}(bdpp)] [bdpp = 2,4-bis(diphenylphosphino)-pentane] in the presence of CO resulted in the formation of methyl acetate and hydrogen as well as a 1:1 mixture of $[PdCl_2(bdpp)]$ and $[Pd_2(\mu\text{-H})(\mu\text{-CO})(bdpp)_2]Cl$.[32] A similar palladium hydride dimer has been isolated and crystallographically characterised by using the ligand 1,3-bis(di-*iso*-propylphosphino)propane.[33]

The formation of **10** from the reaction of **7a** with methanol can be tentatively rationalised as shown in Scheme 2. The methanolysis of the acyl palladium bond in **7a** generates an unstable monomeric or dimeric palladium hydride complex that rapidly decomposes with the formation of **10**, palladium metal and hydrogen. The observed unreactivity of **10** with CO or ethene together with the plausible assumption that reaction of ethene with the palladium hydride complex generated by the methanolysis of complexes similar to **7a** or **9a** is slower than its decomposition makes an efficient chain transfer process for the CO–ethene co-polymerisation catalysed by complex **5a** unavailable. This helps to rationalise the results obtained in the catalytic test reactions.

Conclusions

P,N-Donor ligands containing π-accepting *N*-pyrrolyl groups can be prepared from 7-azaindole in a two-step process involving lithiation followed by reaction with a chlorophosphine. These ligands readily coordinate to palladium(II), platinum(II) and rhodium(I), and both spectroscopic and structural evidence confirm that the di(*N*-pyrrolyl)-substituted ligand $\mathbf{L}^2$ is a stronger π-acceptor/weaker σ-donor than the diphenyl-substituted ligand $\mathbf{L}^1$.

The controlled stepwise insertion reactions of CO and ethene in the palladium methyl complexes **5a**,**b** provided the acyl palladium complexes **7a**,**b** and alkyl complexes **8a**,**b** which were fully characterised. Preliminary catalytic experiments for the CO–ethene co-polymerisation showed that **5a**,**b** are both active catalysts with **5b** affording slightly higher activities. The presence of methanol causes a decrease in activity or catalyst decomposition, and studies on the termination reactions caused by methanol suggested that under the catalytic conditions the decomposition of a palladium hydride intermediate produces a bis(chelate) complex **10** that is responsible for the obtained low activities. A mechanism for the decomposition pathway has been proposed, and **10** has been isolated and crystallographically characterised.

Although the electronic difference between $\mathbf{L}^1$ and $\mathbf{L}^2$ is manifested in structural parameters such as M–P and P–N bond lengths, it does not lead to significant differences in the catalytic activity of their palladium methyl complexes in CO–ethene co-polymerisation. However, differences in reactivity from phosphine–imine compounds have been observed.

Experimental

General experimental

Reactions were routinely carried out using Schlenk-line techniques under pure dry dinitrogen or argon, using dry dioxygen-free solvents unless noted otherwise. Microanalyses (C, H and N) were carried out by Mr Alan Carver (University of Bath Microanalytical Service). Infrared spectra were recorded on a Nicolet 510P spectrometer as KBr pellets, Nujol mulls on KBr discs or in solutions using KBr cells. NMR spectra were recorded on JEOL EX-270, Varian Mercury 400 and Bruker Avance 300 spectrometers referenced to TMS or 85% H_3PO_4. The complexes $[PdCl_2(cod)]$,[34] $[PtCl_2(cod)]$,[35] $[Rh(\mu\text{-Cl})(cod)]_2$ [36] and [PdClMe(cod)] [37] were prepared by standard literature methods. Pyrrole was dried over molecular sieves and distilled before use, and triethylamine was distilled over potassium before use. $PCl(NC_4H_4)_2$ was prepared as described previously.[15,38]

Synthesis of 7-aza-*N*-indolyldiphenylphosphine $\mathbf{L}^1$

A solution of BuLi in hexane (5.0 cm^3, 2.5 M) was added dropwise to a solution of 7-azaindole (1.50 g, 12.7 mmol) in THF–hexane at −78 °C. The reaction mixture was allowed to warm to ambient temperature and stirred for further 30 min. The yellow solution was added dropwise to a cold hexane solution of $PClPh_2$ (2.75 g, 12.5 mmol). After 4 h stirring, the white precipitate was removed by filtration to give a colourless solution. After evaporation of the solvent under reduced pressure the colourless residue was triturated in hexane to give a white powder. The product was recrystallised from dichloromethane–hexane to give $\mathbf{L}^1$. Yield: 2.70g (72%). Calc. for $C_{19}H_{15}N_2P$: C, 75.5; H, 5.00; N, 9.27%. Found: C, 75.1; H, 4.99; N, 9.02%. $^{31}P\{^1H\}$ NMR (161.8 MHz, $CDCl_3$): δ 33.4 (s). ^{1}H NMR (399.8 MHz, $CDCl_3$): δ 8.40 (dd, 1H, $^3J_{HH}$ 4.8 Hz, $^4J_{HH}$ 1.6 Hz, H_6), 7.91 (dm, 1H, $^3J_{HH}$ 8.0 Hz, H_4), 7.40–7.33 (m, 10H, H_o, H_m, H_p), 7.12 (dd, 1H, $^3J_{HH}$ 4.8, 8.0 Hz, H_5), 6.96 (dd, 1H, $^3J_{HH}$ 3.6 Hz, $^3J_{HP}$ 1.8 Hz, H_2), 6.57 (dd, 1H, $^3J_{HH}$ 3.6 Hz, $^4J_{HP}$ 1.2 Hz, H_3). $^{13}C\{^1H\}$ NMR (75.5 MHz, $CDCl_3$): δ 152.9 (d, $^2J_{CP}$ 16 Hz, C_8), 143.9 (s, C_6), 136.6 (d, $^1J_{CP}$ 14 Hz, C_i), 132.6 (d, $^2J_{CP}$ 20 Hz, C_o), 130.3 (d, $^2J_{CP}$ 7 Hz, C_2), 130.0 (s, C_p), 129.2 (s, C_4), 129.0 (d, $^3J_{CP}$ 7 Hz, C_m), 122.4 (s, C_9), 117.1 (s, C_5), 104.9 (s, C_3).

Synthesis of 7-aza-*N*-indolyl-di-*N*-pyrrolyl phosphine $\mathbf{L}^2$

A solution of BuLi in hexane (2.0 cm^3, 2.5 M) was added dropwise to a solution of 7-azaindole (0.61 g, 5.2 mmol) in THF–

hexane at −78 °C. The reaction mixture was allowed to warm to ambient temperature and stirred for further 30 min. The yellow solution was added dropwise to a cold solution of $PCl(NC_4H_4)_2$ (1.03 g, 5.2 mmol) in THF–hexane. After 2 h stirring, the white precipitate which had formed was removed by filtration to give a colourless solution. After evaporation of the solvent under reduced pressure, the colourless residue was washed with cold hexane to obtain **L²** as a colourless oil. Yield: 1.05 g (72%). $^{31}P\{^1H\}$ NMR (161.8 MHz, $CDCl_3$): δ 72.2 (s). ^1H NMR (399.8 MHz, $CDCl_3$): δ 8.36 (dd, 1H, $^3J_{HH}$ 4.8 Hz, $^4J_{HH}$ 1.6 Hz, H_6), 7.91 (ddd, 1H, $^3J_{HH}$ 8.0 Hz, $^4J_{HH}$ 1.6 Hz, $^5J_{HP}$ 1.0 Hz, H_4), 7.16 (dd, 1H, $^3J_{HH}$ 4.8, 8.0 Hz, H_5), 6.89 (*ps*. quin, 4H, *J* 2.0 Hz, H_o), 6.82 (dd, 1H, $^3J_{HH}$ 3.7 Hz, $^3J_{HP}$ 2.4 Hz, H_2), 6.61 (dd, 1H, $^3J_{HH}$ 3.7 Hz, $^4J_{HP}$ 0.6 Hz, H_3), 6.40 (*ps*. t, 4H, *J* 2.0 Hz, H_β). $^{13}C\{^1H\}$ NMR (100.5 MHz, $CDCl_3$): δ 151.5 (d, $^2J_{CP}$ 15 Hz, C_8), 143.9 (s, C_6), 129.1 (s, C_4), 126.8 (d, $^2J_{CP}$ 4.6 Hz, C_2), 122.7 (d, $^2J_{CP}$ 15 Hz, C_o), 122.4 (s, C_9), 117.7 (s, C_5), 113.0 (d, $^3J_{CP}$ 4 Hz, C_β), 106.0 (s, C_3).

Synthesis of [$PdCl_2(L^1$-κ²*P,N*)] 1a

[$PdCl_2$(cod)] (0.230 g, 0.81 mmol) was added to a dichloromethane solution of **L¹** (0.244 g, 0.81 mmol). The solution was stirred for 2 h, then half of the solvent was evaporated under reduced pressure. Upon addition of hexane a yellow precipitate was formed, which was filtered, washed with hexane and dried under reduced pressure. The product was recrystallised from dichloromethane–hexane. Yield 0.379 g (98%). Calc. for $C_{19}H_{15}Cl_2N_2PPd\cdot CH_2Cl_2$: C, 42.6; H, 3.04; N, 4.96%. Found: C, 42.5; H, 3.04; N, 4.96%. $^{31}P\{^1H\}$ NMR (161.8 MHz, $CDCl_3$): δ 80.9 (s). ^1H NMR (399.8 MHz, $CDCl_3$): δ 9.15 (dm, 1H, $^3J_{HH}$ 4.8 Hz, H_6), 8.15 (dm, 1H, $^3J_{HH}$ 8.1 Hz, H_4), 7.90–7.84 (m, 4H, H_m), 7.70–7.64 (m, 2H, H_p), 7.58–7.52 (m, 4H, H_o), 7.32 (dd, 1H, $^3J_{HH}$ 4.8, 8.1 Hz, H_5), 7.17 (dd, 1H, $^3J_{HH}$ 3.7 Hz, $^3J_{HP}$ 2.0 Hz, H_2), 7.01 (d, 1H, $^3J_{HH}$ 3.7 Hz, H_3).

Synthesis of [$PdCl_2(L^2$-κ²*P,N*)] 1b

As for **1a** using [$PdCl_2$(cod)] (0.335 g, 1.2 mmol) and **L²** (0.336 g 1.2 mmol). Yield 0.526 g (98%). Calc. for $C_{15}H_{13}Cl_2N_4PPd$: C, 39.4; H, 2.86; N, 12.2%. Found: C, 39.0; H, 2.74; N, 11.9%. $^{31}P\{^1H\}$ NMR (161.8 MHz, CD_2Cl_2): δ 70.5 (s). ^1H NMR (399.8 MHz, CD_2Cl_2): δ 9.06 (dt, 1H, $^3J_{HH}$ 5.6 Hz, $^4J_{HH}$ 1.2 Hz, $^4J_{HP}$ 1.2 Hz, H_6), 8.21 (ddd, 1H, $^3J_{HH}$ 8.0 Hz, $^4J_{HH}$ 2.8 Hz, $^5J_{HP}$ 1.2 Hz, H_4), 7.43 (dd, 1H, $^3J_{HH}$ 5.6, 8.0 Hz, H_5), 7.34 (*ps*. t, 1H, $^3J_{HH}$ 3.2 Hz, $^3J_{HP}$ 3.2 Hz, H_2), 7.17 (*ps*. quin, H_o), 7.09 (d, 1H, $^3J_{HH}$ 3.2 Hz, H_3), 6.55 (*ps*. t, 4H, H_β).

Synthesis of [$PtCl_2(L^1$-κ²*P,N*)] 2a

[$PtCl_2$(cod)] (0.418 g, 1.1 mmol) was added to a dichloromethane solution of **L¹** (0.338 g, 1.1 mmol). The solution was stirred for 2 h and half of the solvent was evaporated under reduced pressure. Upon addition of hexane a colourless precipitate was formed, which was filtered, washed with hexane and dried under reduced pressure. The product was recrystallised from dichloromethane–hexane. Yield: 0.620 g (98%). Calc. for $C_{19}H_{15}Cl_2N_2PPt\cdot{}^1/_2CH_2Cl_2$: C, 38.4; H, 2.64; N, 4.59%. Found: C, 38.7; H, 2.69; N, 4.67%. $^{31}P\{^1H\}$ NMR (161.8 MHz, CD_2Cl_2): δ 55.4 (s, $^1J_{PPt}$ 4125 Hz). ^1H NMR (399.8 MHz, CD_2Cl_2): δ 9.33 (dd, 1H, $^3J_{HH}$ 5.7 Hz, $^4J_{HH}$ 1.2 Hz, $^3J_{HPt}$ 39 Hz, H_6), 8.21 (dt, 1H, $^3J_{HH}$ 7.8 Hz, $^4J_{HH}$ 1.2 Hz, $^5J_{HP}$ 1.2 Hz, H_4), 7.83–7.78 (m, 4H, H_m), 7.67–7.60 (m, 2H, H_p), 7.58–7.50 (m, 4H, H_o), 7.31 (dd, 1H, $^3J_{HH}$ 7.8, 5.7 Hz, H_5), 7.25 (dd, 1H, $^3J_{HH}$ 3.6 Hz, $^3J_{HP}$ 2.0 Hz, H_2), 7.21 (dd, 1H, $^3J_{HH}$ 3.6 Hz, $^4J_{HP}$ 0.8 Hz, H_3).

Synthesis of [$PtCl_2(L^2$-κ²*P,N*)] 2b

As for **2a** using [$PtCl_2$(cod)] (0.374 g, 1.0 mmol) and **L²** (0.280 g, 1.0 mmol). Yield: 0.535 g (98%). Calc. for $C_{15}H_{13}Cl_2N_4PPt$: C, 33.0; H, 2.40; N, 10.3%. Found: C, 32.8; H, 2.36; N, 10.2%. $^{31}P\{^1H\}$ NMR (121.5 MHz, CD_2Cl_2): δ 47.3 (s, $^1J_{PPt}$ 5409 Hz). ^1H NMR (399.8 MHz, CD_2Cl_2): δ 9.34 (dm, 1H, $^3J_{HH}$ 6.0 Hz, $^3J_{HPt}$ 41 Hz, H_6), 8.26 (ddd, 1H, $^3J_{HH}$ 8.0 Hz, $^4J_{HH}$ 1.2 Hz, $^5J_{HP}$ 2.4 Hz, H_4), 7.42 (dd, 1H, $^3J_{HH}$ 6.0, 8.0 Hz, H_5), 7.37 (dd, $^3J_{HH}$ 3.6 Hz, $^3J_{HP}$ 2.8 Hz, 1H, H_2), 7.28 (dd, 1H, $^3J_{HH}$ 3.2, $^4J_{HP}$ 0.4 Hz, H_3), 7.15 (*ps*. quin, 4H, H_o), 6.53 (*ps*. t, 4H, H_β).

Synthesis of [RhCl(CO)(L^1-κ²*P,N*)] 3a

$[Rh(\mu\text{-}Cl)(cod)]_2$ (0.295 g, 0.60 mmol) was added to a dichloromethane solution of **L¹** (0.362 g, 1.20 mmol). The solution was stirred for 2 h with CO gas bubbling through it. Upon addition of hexane a yellow precipitate was formed, which was separated by filtration, dried under reduced pressure and recrystallised from dichloromethane–hexane. Yield: 0.461 g (82%). Calc. for $C_{20}H_{15}ClN_2OPRh$: C, 51.3; H, 3.23; N, 5.98%. Found: C, 50.9; H, 3.22; N, 5.99%). $^{31}P\{^1H\}$ NMR (161.8 MHz, CD_2Cl_2): δ 104.1 (d, $^1J_{PRh}$ 180 Hz). ^1H NMR (399.8 MHz, CD_2Cl_2): δ 9.03 (dm, 1H, $^3J_{HH}$ 5.2 Hz, H_6), 8.06 (dd, 1H, $^3J_{HH}$ 8.0 Hz, $^4J_{HH}$ 1.2 Hz, H_4), 7.76–7.70 (m, 4H, H_m), 7.58–7.55 (m, 2H, H_p), 7.52–7.47 (m, 4H, H_o), 7.25–7.22 (m, 2H, H_2, H_5), 6.92 (d, 1H, $^3J_{HH}$ 3.6 Hz, H_3). $^{13}C\{^1H\}$ NMR (100.5 MHz, CD_2Cl_2): δ 187.1 (dd, $^1J_{CRh}$ 70 Hz, $^2J_{CP}$ 23 Hz, CO), 156.4 (d, $^2J_{CP}$ 17 Hz, C_8), 142.9 (s, C_6), 132.3 (s, C_p), 132.2 (s, C_4), 132.1 (d, $^2J_{CP}$ 15 Hz, C_o), 131.4 (d, $^1J_{CP}$ 3 Hz, C_i), 129.1 (d, $^3J_{CP}$ 11 Hz, C_m), 125.3 (d, $^2J_{CP}$ 7 Hz, C_2), 120.0 (d, $^3J_{CP}$ 6 Hz, C_9), 117.5 (s, C_5), 110.7 (s, C_3). IR (CH_2Cl_2, cm^{-1}): 2005 [s, *ν*(CO)]. IR (KBr, cm^{-1}): 1992 [s, *ν*(CO)].

Synthesis of [RhCl(CO)(L^2-κ²*P,N*)] 3b

As for **3a** using $[Rh(\mu\text{-}Cl)(cod)]_2$ (0.352 g, 0.71 mmol) and **L²** (0.400 g 1.43 mmol). Yield: 0.533 g (84%). Calc. for $C_{16}H_{13}Cl_2N_4OPRh$: C, 43.0; H, 2.93; N, 12.5%. Found: C, 43.1; H, 2.91; N, 12.6%. $^{31}P\{^1H\}$ NMR (161.8 MHz, CD_2Cl_2): δ 101.9 (d, $^1J_{PRh}$ 242 Hz). ^1H NMR (399.8 MHz, CD_2Cl_2): δ 8.94 (dm, 1H, $^3J_{HH}$ 5.6 Hz, H_6), 8.13 (ddd, 1H, $^3J_{HH}$ 8.0 Hz, $^4J_{HH}$ 1.2 Hz, $^5J_{HP}$ 2.0 Hz, H_4), 7.39 (t, 1H, $^3J_{HH}$ 3.2 Hz, $^3J_{HP}$ 5.6 Hz, H_2), 7.32 (dd, 1H, $^3J_{HH}$ 5.6, 8.0 Hz, H_5), 7.09 (*ps*. quin, 4H, H_o), 6.97 (d, 1H, $^3J_{HH}$ 3.2 Hz, H_3), 6.49 (m, 4H, H_β). $^{13}C\{^1H\}$ NMR (100.5 MHz, CD_2Cl_2): δ 186.1 (dd, $^1J_{CRh}$ 70 Hz, $^2J_{CP}$ 23 Hz, CO), 155.8 (d, $^2J_{CP}$ 25 Hz, C_8), 143.2 (s, C_6), 133.4 (s, C_4), 124.7 (d, $^2J_{CP}$ 8 Hz, C_2), 124.0 (d, $^2J_{CP}$ 10 Hz, C_o), 120.4 (d, $^3J_{CP}$ 10 Hz, C_9), 118.8 (s, C_5), 115.4 (d, $^3J_{CP}$ 10 Hz, C_β), 112.1 (d, $^3J_{CP}$ 2 Hz, C_3). IR (CH_2Cl_2, cm^{-1}): 2027 [s, *ν*(CO)]. IR (KBr, cm^{-1}): 2017 [s, *ν*(CO)].

Synthesis of [PdClMe(L^1-κ²*P,N*)] 4a

[PdClMe(cod)] (0.406 g, 1.53 mmol) was added to a dichloromethane solution of **L¹** (0.463 g, 1.53 mmol). The pale yellow solution was stirred for 2 h and half of the solvent was eliminated under reduced pressure. Hexane was added to precipitate a white powder which was isolated by filtration, washed with hexane then diethyl ether and dried under reduced pressure. Yield: 0.680 g (97%). Calc. for $C_{20}H_{18}ClN_2PPd\cdot{}^1/_3CH_2Cl_2$: C, 50.1; H, 3.86; N, 5.75%. Found: C, 49.8; H, 3.94; N, 5.75%. $^{31}P\{^1H\}$ NMR (161.8 MHz, CD_2Cl_2): δ 83.0 (s). ^1H NMR (399.8 MHz, CD_2Cl_2): δ 8.75 (dd, 1H, $^3J_{HH}$ 5.2 Hz, $^4J_{HH}$ 1.6 Hz, H_6), 8.05 (dt, 1H, $^3J_{HH}$ 8.0 Hz, $^4J_{HH}$ 1.6 Hz, $^5J_{HP}$ 1.6 Hz, H_4), 7.68–7.63 (m, 4H, H_m), 7.61–7.56 (m, 2H, H_p), 7.52–7.46 (m, 4H, H_o), 7.26 (dd, 1H, $^3J_{HH}$ 5.2, 8.0 Hz, H_5), 7.18 (dd, 1H, $^3J_{HH}$ 4.0 Hz, $^3J_{HP}$ 2.0 Hz, H_2) 6.84 (d, 1H, $^3J_{HH}$ 4.0 Hz, H_3), 0.75 (d, 3H, $^3J_{HP}$ 4.4 Hz, Me). $^{13}C\{^1H\}$ NMR (75.5 MHz, CD_2Cl_2) δ 155.2 (d, $^2J_{CP}$ 15 Hz, C_8), 142.8 (s, C_6), 133.2 (d, $^2J_{CP}$ 14 Hz, C_o), 133.0 (d, $^1J_{CP}$ 2 Hz, C_i), 131.7 (s, C_p), 130.0 (s, C_4), 129.6 (d, $^3J_{CP}$ 11 Hz, C_m), 126.2 (d, $^2J_{CP}$ 7 Hz, C_2), 120.8 (d, $^3J_{CP}$ 6 Hz, C_9), 118.6 (s, C_5), 110.8 (s, C_3), −5.8 (d, $^2J_{CP}$ 5 Hz, Me).

Synthesis of [PdClMe(L^2-κ²*P,N*)] 4b

As for **4a** using [PdClMe(cod)] (1.40 g, 5.3 mmol) and **L²** (1.47 g, 5.3 mmol). Yield 1.93 g (84%). Calc. for $C_{16}H_{16}ClN_4$-

PPd: C, 44.0; H, 3.69; N, 12.8%. Found: C, 43.4; H, 3.55; N, 12.7%. $^{31}P\{^1H\}$ NMR (161.8 MHz, CD_2Cl_2): δ 89.3 (s). ^1H NMR (399.8 MHz, CD_2Cl_2): δ 8.73 (dd, 1H, $^3J_{HH}$ 5.2 Hz, $^4J_{HH}$ 0.8 Hz, H_6), 8.11 (ddd, 1H, $^3J_{HH}$ 7.2 Hz, $^4J_{HH}$ 0.8 Hz, $^5J_{HP}$ 1.2 Hz, H_4), 7.36 (dd, 1H, $^3J_{HH}$ 5.6, 7.2 Hz, H_5), 7.35 (d, 1H, $^3J_{HH}$ 4.4 Hz, H_2), 7.03 (*ps*. quin, 4H, H_α), 6.92 (d, 1H, $^3J_{HH}$ 4.4 Hz, H_3), 6.49 (m, 4H, H_β), 0.95 (d, 3H, $^3J_{HP}$ 3.6 Hz, Me). $^{13}C\{^1H\}$ NMR (100.5 MHz, CD_2Cl_2) δ 154.2 (d, $^2J_{CP}$ 20 Hz, C_8), 143.0 (s, C_6), 132.3 (s, C_4), 124.8 (d, $^2J_{CP}$ 7 Hz, C_2), 124.0 (d, $^2J_{CP}$ 8 Hz, C_α), 120.7 (d, $^2J_{CP}$ 7 Hz, C_9), 119.6 (s, C_5), 115.6 (d, $^3J_{CP}$ 8 Hz, C_β), 111.9 (d, $^2J_{CP}$ 3 Hz, C_3), −4.6 (d, $^2J_{CP}$ 5 Hz, Me).

Synthesis of [PdMe(OTf)(L^1-κ^2*P,N*)] 5a

AgOTf (0.095 g, 0.37 mmol) was added to a dichloromethane solution of **4a** (0.170 g, 0.37 mmol). After 4 h stirring the suspension was filtered to remove AgCl and the filtrate evaporated to dryness. The resulting pale yellow powder was washed with hexane and dried under reduced pressure. Yield: 0.192 g (91%). Calc. for $C_{21}H_{18}F_3N_2O_3PPdS$: C, 44.0; H, 3.17; N, 4.89%. Found: C, 43.8; H, 3.16; N, 4.76%. $^{31}P\{^1H\}$ NMR (161.8 MHz, CD_2Cl_2): δ 84.6 (s). ^1H NMR (399.8 MHz, CD_2Cl_2): δ 8.53 (d, 1H, $^3J_{HH}$ 5.6 Hz, H_6), 8.07 (d, 1H, $^3J_{HH}$ 7.9 Hz, H_4), 7.82–7.46 (m, 6H, H_m, H_p), 7.54 (m, 4H, H_o), 7.32 (dd, 1H, $^3J_{HH}$ 5.6, 7.9 Hz, H_5), 7.16 (dd, 1H, $^3J_{HH}$ 2.4 Hz, $^3J_{HP}$ 3.6 Hz, H_2), 6.86 (d, 1H, $^3J_{HH}$ 3.6 Hz, H_3), 0.85 (d, 3H, $^3J_{HP}$ 1.6 Hz, Me). $^{13}C\{^1H\}$ NMR (67.9 MHz, CD_2Cl_2): δ 154.8 (d, $^2J_{CP}$ 15 Hz, C_8), 142.9 (s, C_6), 133.7 (s, C_p), 133.3 (d, $^2J_{CP}$ 15 Hz, C_o), 132.5 (s, C_i), 130.0 (d, $^3J_{CP}$ 12 Hz, C_m), 129.9 (s, C_4), 126.4 (d, $^2J_{CP}$ 6 Hz, C_2), 121.1 (d, $^3J_{CP}$ 6 Hz, C_9), 119.1 (s, C_5), 111.4 (s, C_3), −1.2 (d, $^2J_{CP}$ 4 Hz, Me). $^{19}F\{^1H\}$ NMR (376.2 MHz, CD_2Cl_2): δ –78.9 (s).

Synthesis of [PdMe(OTf)(L^2-κ^2*P,N*)] 5b

As for **5a** using AgOTf (0.095 g, 0.37 mmol) and **4b** (0.163 g, 0.37 mmol). Yield: 0.202 g, (98%). Calc. for $C_{17}H_{16}F_3N_4O_3PPdS$: C, 37.1; H, 2.93; N, 10.2%. Found: C, 37.1; H, 2.98; N, 10.1%. $^{31}P\{^1H\}$ NMR (161.8 MHz, CD_2Cl_2): δ 90.1 (s). ^1H NMR (399.8 MHz, CD_2Cl_2): δ 8.48 (bd, 1H, $^3J_{HH}$ 5.6 Hz, H_6), 8.16 (dm, 1H, $^3J_{HH}$ 8.0 Hz, H_4), 7.40 (dd, 1H, $^3J_{HH}$ 5.6, 8.0 Hz, H_5), 7.36 (*ps*. t, 1H, $^3J_{HH}$ 3.6 Hz, $^3J_{HP}$ 3.6 Hz, H_2), 7.04 (*ps*. quin, 4H, H_α), 6.95 (d, 1H, $^3J_{HH}$ 3.6 Hz, H_3), 6.54 (m, 4H, H_β), 1.04 (s, 3H, Me). $^{13}C\{^1H\}$ NMR (100.5 MHz, CD_2Cl_2): δ 153.8 (d, $^2J_{CP}$ 19 Hz, C_8), 143.4 (s, C_6), 133.1 (s, C_4), 125.0 (d, $^2J_{CP}$ 6 Hz, C_2), 124.2 (d, $^2J_{CP}$ 9 Hz, C_α), 121.2 (d, $^3J_{CP}$ 8 Hz, C_9), 120.2 (s, C_5), 116.4 (d, $^3J_{CP}$ 9 Hz, C_β), 112.5 (d, $^3J_{CP}$ 4 Hz, C_3), 0.6 (s, Me). $^{19}F\{^1H\}$ NMR (376.2 MHz, CD_2Cl_2): δ −78.5 (s).

Synthesis of [PdCl{C(O)Me}(L^1-κ^2*P,N*)] 6a

Compound **4a** (0.078 g, 0.17 mmol) was transferred into a NMR tube fitted with a Young valve and dissolved in a minimum amount of CD_2Cl_2. A CO pressure of approximately 10 psi was applied and the NMR tube was shaken vigorously. After 48 h the solution was transferred into a small Schlenk and hexane added to precipitate a pale yellow powder. This was isolated by filtration and dried under reduced pressure. Yield: 0.057 g (69%). Calc. for $C_{21}H_{18}ClN_2OPPd\cdot{}^1/_4CH_2Cl_2$: C, 50.2; H, 3.67; N, 5.51%. Found: C, 50.2; H, 3.64; N, 5.51%. $^{31}P\{^1H\}$ NMR (161.8 MHz, $CDCl_3$): δ 64.9 (s). ^1H NMR (399.8 MHz, $CDCl_3$): δ 8.68 (d, 1H, $^3J_{HH}$ 5.2 Hz, H_6), 8.04 (d, 1H, $^3J_{HH}$ 7.8 Hz, H_4), 7.71–7.66 (m, 4H, H_m), 7.61–7.58 (m, 2H, H_p), 7.55–7.50 (m, 4H, H_o), 7.28 (dd, 1H, $^3J_{HH}$ 5.2, 7.8 Hz, H_5), 7.17 (dd, 1H, $^3J_{HH}$ 3.6 Hz, $^3J_{HP}$ 2.4 Hz, H_2), 6.82 (d, 1H, $^3J_{HH}$ 3.6 Hz, H_3), 2.34 (s, 3H, Me). $^{13}C\{^1H\}$ NMR (100.5 MHz, CD_2Cl_2): δ 224.3 (d, $^2J_{CP}$ 6 Hz, CO), 154.8 (d, $^2J_{CP}$ 21 Hz, C_8), 143.2 (s, C_6), 133.5–130.0 (m, C_i, C_o, C_m, C_p, C_4), 127.0 (d, $^2J_{CP}$ 9 Hz, C_2), 121.5 (d, $^3J_{CP}$ 8 Hz, C_9), 119.1 (s, C_5), 110.9 (s, C_3), 39.0 (d, $^3J_{CP}$ 30 Hz, Me). IR (KBr, cm^{-1}): 1697 [s, ν(CO)].

Synthesis of [PdCl{C(O)Me}(L^2-κ^2*P,N*)] 6b

Compound **4b** (0.050 g, 0.11 mmol) was transferred in a NMR tube fitted with a Young valve and dissolved in a minimum amount of CD_2Cl_2. A CO pressure of approximately 20 psi was applied and the NMR tube was shaken vigorously. After 2 h $^{31}P\{^1H\}$ NMR spectroscopy indicated a conversion of approximately 40%. $^{31}P\{^1H\}$ NMR (161.8 MHz, CD_2Cl_2): δ 78.9 (s). ^1H NMR (399.8 MHz, CD_2Cl_2): δ 8.53 (bd, 1H, $^3J_{HH}$ 4.8 Hz, H_6), 8.12 (m, 1H, H_4), 7.40 (m, 1H, H_5), 7.37 (m, 1H, H_3), 7.05 (*ps.* quin, 4H, H_α), 6.90 (d, 1H, $^3J_{HH}$ 3.6 Hz, H_2), 6.51 (m, 4H, H_β), 2.09 (s, 3H, Me). $^{13}C\{^1H\}$ NMR (100.5 MHz, CD_2Cl_2): δ 219.3 (s, CO), 153.8 (d, $^2J_{CP}$ 18 Hz, C_8), 142.9 (s, C_6), 132.5 (s, C_4), 125.1 (d, $^2J_{CP}$ 8 Hz, C_2), 124.0 (d, $^2J_{CP}$ 11 Hz, C_α), 121.0 (d, $^3J_{CP}$ 4 Hz, C_9), 119.7 (s, C_5), 115.8 (d, $^3J_{CP}$ 9 Hz, C_β), 111.9 (s, C_3), 39.6 (d, $^3J_{CP}$ 32 Hz, Me). IR (CH_2Cl_2, cm^{-1}): 1715 [s, ν(CO)].

Synthesis of [Pd{C(O)Me}(OTf)(L^1-κ^2*P,N*)] 7a

Compound **5a** (0.050 g, 0.087 mmol) was transferred into a NMR tube fitted with a Young valve and dissolved in a minimum amount of CD_2Cl_2. A CO pressure of approximately 20 psi was applied and the NMR tube was shaken vigorously. After ~5 min $^{31}P\{^1H\}$ NMR spectroscopy showed complete conversion to **7a**. The contents of the NMR tube were transferred into a Schlenk and a sample was taken to record the IR spectrum. The solution was diluted with dichloromethane and layered with hexane. Slow diffusion of hexane into the dichloromethane solution gave **7a** as colourless crystals suitable for X-ray diffraction studies. $^{31}P\{^1H\}$ NMR (161.8 MHz, CD_2Cl_2): δ 65.5 (s). ^1H NMR (399.8 MHz, CD_2Cl_2): δ 8.46 (d, 1H, $^3J_{HH}$ 5.2 Hz, H_6), 8.11 (d, 1H, $^3J_{HH}$ 8.0 Hz, H_4), 7.71–7.64 (m, 6H, H_o, H_p), 7.57–7.52 (m, 4H, H_m), 7.30 (dd, 1H, $^3J_{HH}$ 5.2, 8.0 Hz, H_5), 7.20 (dd, 1H, $^3J_{HH}$ 3.6 Hz, $^3J_{HP}$ 2.4 Hz, H_2), 6.86 (d, 1H, $^3J_{HH}$ 3.6 Hz, H_3), 2.27 (d, 3H, $^4J_{HP}$ 1.2 Hz, Me). $^{13}C\{^1H\}$ NMR (100.5 MHz, CD_2Cl_2): δ 220.1 (d, $^2J_{CP}$ 6 Hz, CO), 152.5 (d, $^2J_{CP}$ 14 Hz, C_8), 142.8 (s, C_6), 133.5 (d, $^1J_{CP}$ 2 Hz, C_i), 133.1 (d, $^2J_{CP}$ 15 Hz, C_o), 132.6 (s, C_p), 129.9 (d, $^3J_{CP}$ 12 Hz, C_m), 127.6 (s, C_4), 126.6 (d, $^2J_{CP}$ 6 Hz, C_2), 121.6 (d, $^3J_{CP}$ 5 Hz, C_9), 119.0 (s, C_5), 110.8 (s, C_3), 36.5 (d, $^3J_{CP}$ 29 Hz, Me). $^{19}F\{^1H\}$ NMR (376.2 MHz, CD_2Cl_2): δ −78.7 (s). IR (CD_2Cl_2, cm^{-1}): 1711 [s, ν(CO)].

Synthesis of [Pd{C(O)Me}(OTf)(L^2-κ^2*P,N*)] 7b

As for **7a** starting from **5b** (0.050 g, 0.091 mmol). $^{31}P\{^1H\}$ NMR (161.8 MHz, CD_2Cl_2): δ 79.1 (s). ^1H NMR (399.8 MHz, CD_2Cl_2): δ 8.37 (bd, 1H, $^3J_{HH}$ 5.2 Hz, H_6), 8.11 (dm, 1H, $^3J_{HH}$ 8.0 Hz, H_4), 7.42 (*ps*. t, 1H, $^3J_{HH}$ 3.5 Hz, $^3J_{HP}$ 3.5 Hz, H_2), 7.39 (dd, 1H, $^3J_{HH}$ 5.2, 8.0 Hz, H_5), 7.09–7.07 (m, 4H, H_α), 6.93 (d, 1H, $^3J_{HH}$ 3.5 Hz, H_3), 6.57–6.55 (m, 4H, H_β), 2.18 (d, 3H, $^4J_{HP}$ 3.2 Hz, Me). $^{13}C\{^1H\}$ NMR (100.5 MHz, CD_2Cl_2): δ 216.5 (d, $^2J_{CP}$ 12 Hz, CO), 153.3 (d, $^2J_{CP}$ 20 Hz, C_8), 143.7 (s, C_6), 133.1 (s, C_4), 125.2 (d, $^2J_{CP}$ 7 Hz, C_2), 124.0 (d, $^2J_{CP}$ 10 Hz, C_α), 121.7 (d, $^3J_{CP}$ 7 Hz, C_9), 120.2 (s, C_5), 116.4 (d, $^3J_{CP}$ 8 Hz, C_β), 112.0 (d, $^3J_{CP}$ 3 Hz, C_3), 36.6 (d, $^3J_{CP}$ 46 Hz, Me). $^{19}F\{^1H\}$ NMR (376.2 MHz, CD_2Cl_2): δ −78.2 (s). IR (CD_2Cl_2, cm^{-1}): 1729 [s, ν(CO)].

Synthesis of [Pd{$CH_2CH_2C(O)Me$-κ^2*C,O*}(L^1-κ^2*P,N*)]OTf 8a

Compound **5a** (0.050 g, 0.087 mmol) was transferred to a NMR tube fitted with a Young valve and dissolved in a minimum amount of CD_2Cl_2. A CO pressure of approximately 20 psi was applied and the NMR tube was shaken vigorously. After 20 min the NMR tube was immersed in liquid nitrogen and placed under reduced pressure. After 10 min the Young valve was closed and the NMR tube was left to reach ambient temperature. This operation was repeated three times in order to eliminate unreacted CO. A C_2H_4 pressure of approximately 10 psi was applied and the NMR tube was shaken vigorously every 10 min for 1 h. After this time the $^{31}P\{^1H\}$ NMR spectrum

showed complete conversion of **5a** to **8a**. The contents of the NMR tube were transferred in a Schlenk, and a small sample taken to record an IR spectrum. Dichloromethane was added and the solution was layered with hexane. The two solvents slowly mixed overnight allowing **8a** to precipitate out as crystals suitable for X-ray crystallography. $^{31}P\{^1H\}$ NMR (161.8 MHz, CD_2Cl_2): δ 84.3 (s). ^1H NMR (399.8 MHz, CD_2Cl_2): δ 8.45 (d, 1H, $^3J_{HH}$ 5.2 Hz, H_6), 8.19 (ddd, 1H, $^3J_{HH}$ 8.0 Hz, $^4J_{HH}$ 1.2 Hz, $^5J_{HP}$ 1.2 Hz, H_4), 7.69–7.62 (m, 6H, H_p, H_o), 7.60–7.47 (m, 4H, H_m), 7.39 (dd, 1H, $^3J_{HH}$ 5.2, 8.0 Hz, H_5), 7.24 (dd, 1H, $^3J_{HH}$ 3.2 Hz, $^3J_{HP}$ 2.0 Hz, H_2), 6.95 (d, 1H, $^3J_{HH}$ 3.2 Hz, H_3), 3.16 (t, 2H, $^3J_{HH}$ 6.2 Hz, CH_2CO), 2.49 (s, 3H, Me), 1.99 (dt, 2H, $^3J_{HH}$ 6.2 Hz, $^3J_{HP}$ 1.2 Hz, CH_2Pd). $^{13}C\{^1H\}$ NMR (100.5 MHz, CD_2Cl_2): δ 222.4 (d, $^3J_{CP}$ 8 Hz, CO), 154.5 (d, $^2J_{CP}$ 14 Hz, C_8), 143.2 (s, C_6), 133.6 (s, C_4), 133.1 (d, $^2J_{CP}$ 20 Hz, C_o), 132.8 (s, C_p), 132.0 (s, C_i), 126.8 (d, $^2J_{CP}$ 7 Hz, C_2), 130.0 (d, $^3J_{CP}$ 16 Hz, C_m), 121.7 (s, C_9), 119.1 (s, C_5), 111.0 (s, C_3), 51.6 (s, CH_2CO), 28.3 (d, $^4J_{CP}$ 3 Hz, Me), 20.9 (d, $^2J_{CP}$ 2 Hz, CH_2Pd). $^{19}F\{^1H\}$ NMR (376.2 MHz, CD_2Cl_2): δ −79.1 (s). IR (CD_2Cl_2, cm^{-1}): 1631 [s, ν(CO)].

Synthesis of [Pd{$CH_2CH_2C(O)Me$-κ^2*C,O*}(L^2-κ^2*P,N*)]OTf 8b

As for **8a** using compound **5b** (0.050 g, 0.091 mmol). $^{31}P\{^1H\}$ NMR (161.8 MHz, CD_2Cl_2): δ 91.1 (s). ^1H NMR (399.8 MHz, CD_2Cl_2): δ 8.45 (dd, 1H, $^3J_{HH}$ 5.2 Hz, $^4J_{HH}$ 1.2 Hz, H_6), 8.23 (ddd, 1H, $^3J_{HH}$ 8.0 Hz, $^5J_{HP}$ 2.4 Hz, $^4J_{HH}$ 1.2 Hz, H_4), 7.48 (dd, 1H, $^3J_{HH}$ 5.2, 8.0 Hz, H_5), 7.40 (*ps*. t, 1H, $^3J_{HH}$ 3.9 Hz, $^3J_{HP}$ 3.9 Hz, H_2), 7.05 (*ps*. quin, 4H, H_a) 7.02 (d, 1H, $^3J_{HH}$ 3.9 Hz, H_3), 6.58–6.56 (m, 4H, H_β), 3.29–3.25 (m, 2H, CH_2-CO), 2.55 (s, 3H, Me), 2.21–2.17 (m, 2H, CH_2Pd). $^{13}C\{^1H\}$ NMR (75.5 MHz, CD_2Cl_2): δ 237.9 (s, CO), 154.9 (d, $^2J_{CP}$ 15 Hz, C_8), 144.7 (s, C_6), 134.8 (s, C_4), 126.3 (d, $^2J_{CP}$ 6 Hz, C_2), 125.1 (d, $^2J_{CP}$ 10 Hz, C_a), 122.7 (d, $^3J_{CP}$ 7 Hz, C_9), 121.6 (s, C_5), 117.9 (d, $^3J_{CP}$ 9 Hz, C_β), 114.0 (d, $^3J_{CP}$ 4 Hz, C_3), 52.8 (s, CH_2CO), 29.3 (d, $^4J_{CP}$ 3 Hz, Me), 22.9 (s, CH_2Pd). $^{19}F\{^1H\}$ NMR (376.2 MHz, CD_2Cl_2): δ −79.3 (s). IR (CD_2Cl_2, cm^{-1}): 1628 [s, ν(CO)].

Synthesis of [Pd{$C(O)CH_2CH_2C(O)Me$-κ^2*C,O*}(L^1-κ^2*P,N*)]-OTf 9a

A CD_2Cl_2 solution of **8a** (0.055 g, 0.087 mmol) was transferred into a NMR tube fitted with a Young valve and a CO pressure of approximately 10 psi was applied. After 24 h at ambient temperature $^{31}P\{^1H\}$ NMR spectroscopy showed complete conversion of **8a** into **9a**. $^{31}P\{^1H\}$ NMR (161.8 MHz, CD_2Cl_2): δ 69.0 (s). ^1H NMR (399.8 MHz, CD_2Cl_2): δ 8.42 (bd, 1H, $^3J_{HH}$ 5.2 Hz, H_6), 8.15 (dt, 1H, $^3J_{HH}$ 8.0 Hz, $^4J_{HH}$ 1.6 Hz, $^5J_{HP}$ 1.6 Hz, H_4), 7.72–7.64 (m, 6H, H_p, H_o), 7.58–7.53 (m, 4H, H_m), 7.38 (dd, 1H, $^3J_{HH}$ 5.2, 8.0 Hz, H_5), 7.16 (dd, 1H, $^3J_{HH}$ 3.6 Hz, $^3J_{HP}$ 2.0 Hz, H_2), 6.87 (dd, 1H, $^3J_{HH}$ 3.6 Hz, $^4J_{HP}$ 0.6 Hz, H_3), 2.86–2.75 (m, 4H, CH_2), 2.46 (s, 3H, Me). $^{13}C\{^1H\}$ NMR (100.5 MHz, $CDCl_3$): δ 219.1 (s, CO), 217.3 (s, CO), 154.1 (d, $^2J_{CP}$ 14 Hz, C_8), 142.6 (s, C_6), 133.6 (d, $^4J_{CP}$ 3 Hz, C_4), 133.3 (d, $^2J_{CP}$ 15 Hz, C_o), 132.9 (s, C_p), 129.7 (d, $^3J_{CP}$ 13 Hz, C_m), 127.1 (d, $^1J_{CP}$ 7 Hz, C_i), 126.7 (d, $^2J_{CP}$ 6 Hz, C_2), 121.6 (d, $^3J_{CP}$ 4 Hz, C_9), 119.1 (s, C_5), 110.7 (s, C_3), 40.1 (d, $^4J_{CP}$ 25 Hz, Me), 38.2 (s, $PdC(O)CH_2$), 31.2 (s, $COCH_2$). $^{19}F\{^1H\}$ NMR (376.2 MHz, CD_2Cl_2): δ −79.2 (s). IR (CD_2Cl_2, cm^{-1}): 1711, 1622 [s, ν(C=O)].

Synthesis of [Pd{$C(O)CH_2CH_2C(O)Me$-κ^2*C,O*}(L^2-κ^2*P,N*)]-OTf 9b

As for **9a** using compound **8b** (0.055 g, 0.091 mmol). $^{31}P\{^1H\}$ NMR (161.8 MHz, CD_2Cl_2): δ 78.9 (s). ^1H NMR (399.8 MHz, CD_2Cl_2): δ 8.45 (dd, 1H, $^3J_{HH}$ 5.2 Hz, $^4J_{HH}$ 1.2 Hz, H_6), 8.23 (ddd, 1H, $^3J_{HH}$ 8.0 Hz, $^5J_{HP}$ 2.4 Hz, $^4J_{HH}$ 1.2 Hz, H_4), 7.47 (dd, 1H, $^3J_{HH}$ 5.2, 8.0 Hz, H_5), 7.42 (*ps*. t, 1H, $^3J_{HH}$ 3.9 Hz, $^5J_{HP}$ 3.9 Hz, H_2), 7.05 (*ps*. quin, 4H, H_a), 7.02 (d, 1H, $^3J_{HH}$ 3.9 Hz, H_3), 6.57–6.56 (m, 4H, H_β), 2.75–2.74 (m, 4H, CH_2), 2.20 (s, 3H, Me). $^{19}F\{^1H\}$ NMR: δ −78.8 (s). IR (CD_2Cl_2, cm^{-1}): 1716, 1660, [s, ν(C=O)].

Synthesis of [Pd(L^1-κ^2*P,N*)]$(OTf)_2$ 10

AgOTf (0.350 g, 1.36 mmol) was added to a dichloromethane solution of [$PdCl_2$(cod)] (0.165 g, 0.58 mmol) and $\mathbf{L^1}$ (0.392 g, 1.30 mmol). The reaction mixture was stirred for 4 h with the formation of a white precipitate of AgCl. The solid was removed by filtration and the solvent eliminated under reduced pressure. The resulting powder was washed with small amounts of dichloromethane. Crystallisation by slow diffusion of hexane into a dichloromethane solution gave **10** as colourless crystals. Yield: 0.520 g (89%). Calc. for $C_{40}H_{30}F_6N_4O_6P_2PdS_2\cdot{}^3/_2$-$CH_2Cl_2$: C, 43.9; H, 2.93; N, 4.93%. Found: C, 43.7; H, 2.95; N, 4.99%. $^{31}P\{^1H\}$ NMR (161.8 MHz, CD_2Cl_2): δ 90.2 (s). ^1H NMR (399.8 MHz, $CDCl_3$): δ 8.82 (m, 2H, H_6), 8.28 (dd, 2H, $^3J_{HH}$ 8.0 Hz, $^4J_{HH}$ 1.1 Hz, H_4), 7.74–7.68 (m, 8H, H_o), 7.60 (dd, 2H, $^3J_{HH}$ 6.4, 8.0 Hz, H_5), 7.55–7.52 (m, 4H, H_p), 7.36–7.30 (m, 8H, H_m), 7.09–7.07 (m, 2H, H_2), 7.02 (d, 1H, $^3J_{HH}$ 3.6 Hz, H_3). $^{19}F\{^1H\}$ NMR (376.2 MHz, CD_2Cl_2): δ −79.5 (s).

Synthesis of [Pt(L^1-κ^2*P,N*)$_2$]$(OTf)_2$ 11

AgOTf (0.133 g, 0.52 mmol) was added to a dichloromethane solution of **2a** (0.150 g, 0.26 mmol) and $\mathbf{L^1}$ (0.080 g, 0.26 mmol). The reaction mixture was stirred for 4 h with the formation of a white precipitate of AgCl. The solid was removed by filtration and hexane added to precipitate a white powder which was separated by filtration, washed with hexane and dried under reduced pressure. Yield: 0.260g (90%). Calc. for $C_{40}H_{30}$-$F_6N_4O_6P_2PtS_2\cdot{}^1/_4CH_2Cl_2$: C, 43.2; H, 2.75; N, 5.01%. Found: C, 43.2; H, 2.83; N, 5.01%. $^{31}P\{^1H\}$ NMR (161.8 MHz, CD_2Cl_2): δ 62.8 (s, $^1J_{PPt}$ 3601 Hz). ^1H NMR (399.8 MHz, $CDCl_3$): δ 8.96 (br, 2H, H_6), 8.36 (d, 2H, $^3J_{HH}$ 8.0 Hz, H_4), 7.69–7.61 (m, 8H, H_o), 7.54–7.45 (m, 6H, H_5, H_p), 7.35–7.31 (m, 8H, H_m), 7.21–7.17 (m, 2H, H_2), 7.04–7.02 (m, 2H, H_3). $^{19}F\{^1H\}$ NMR (376.2 MHz, CD_2Cl_2): δ −79.4 (s).

Catalytic experiments

The co-polymerisation reactions were carried out in a 500 cm^3 Buchi glass autoclave equipped with a magnetic stirring bar. The catalysts (**5a**,**b**) were transferred *via* cannula under an atmosphere of nitrogen. Dried methanol or TfOH were added using common syringe techniques. The autoclave was pressurised first with C_2H_4 and then with CO. For the reactions at 50 °C, the autoclave was heated in an oil bath. After the appropriate reaction times the pressure was released and the polymer removed by filtration, washed thoroughly with dichloromethane and dried under reduced pressure. Analysis of PK: mp 240–260 °C. ^1H NMR (399.8 MHz, HFIA/C_6D_6): δ 2.69 (br, CH_2CH_2). $^{13}C\{^1H\}$ NMR (100.5 MHz, HFIA/C_6D_6): δ 213.1 (s, CO), 36.1 (s, CH_2). IR (KBr, cm^{-1}): 1695 [s, ν(C=O)].

Crystallography

Crystallographic data for compounds **1a**,**b**, **3a**,**b**, **7a**,**b**, **8a**,**b** and **10** are summarised in Table 7. All data were collected using a Nonius KappaCCD diffractometer with the exception of **1a** which were collected on an Enraf-Nonius CAD4. Full matrix anisotropic refinement was implemented in the final least-squares cycles for all structures with the specific exceptions described below. All data were corrected for Lorentz and polarisation. Extinction corrections were applied in all cases except for **8b**.

Absorption corrections (multiscan) were applied on the basis of their individual merits to data for **3a**, **3b** and **10** (maximum, minimum transmission factors were 1.04, 0.79; 0.80, 0.70; and 1.09, 0.89, respectively). Hydrogen atoms were included at calculated positions throughout with the exceptions described below.

Table 7 Crystallographic data for complexes **1a**,**b**, **3a**,**b**, **7a**,**b**, **8a**,**b** and **10**

Compound	**1a**	**1b**	**3a**	**3b**	**7a**	**7b**	**8a**	**8b**	**10**
Formula	$C_{19}H_{15}Cl_2N_2PPd$	$C_{15}H_{13}Cl_2N_4PPd$	$C_{20}H_{15}ClN_2OPRh$	$C_{16}H_{13}ClN_4OPRh$	$C_{22}H_{18}F_3N_2O_4PPdS$	$C_{18}H_{16}F_3N_4O_4PPdS$	$C_{24}H_{22}F_3N_2O_4PPdS$	$C_{20}H_{20}F_3N_4O_4PPdS$	$C_{40}H_{33}F_6N_4O_{7.50}P_2PdS_2$
M	479.60	457.56	468.67	446.63	600.81	578.78	628.87	606.83	1036.16
T/K	170(2)	150(2)	293(2)	150(2)	150(2)	150(2)	150(2)	150(2)	150(2)
Crystal system	Monoclinic	Monoclinic	Triclinic	Monoclinic	Triclinic	Triclinic	Triclinic	Triclinic	Monoclinic
Space group	$P2_1/c$	$P2_1/c$	$P-1$	$P2_1/c$	$P-1$	$P-1$	$P-1$	$P-1$	$P2_1/n$
a/Å	9.849(2)	8.7400(1)	9.0020(2)	8.7130(1)	9.2280(1)	11.4130(1)	8.2910(1)	8.3530(2)	13.4210(2)
b/Å	15.522(2)	10.8700(1)	13.8360(4)	11.0150(2)	9.3830(2)	13.4650(2)	11.8690(2)	11.2230(4)	20.4340(3)
c/Å	12.376(2)	17.4600(2)	15.0090(4)	17.8380(2)	14.8820(2)	21.9600(3)	13.8810(3)	13.7950(5)	15.6820(2)
α/°	90	90	85.7660(11)	90	77.7580(8)	88.8130(5)	71.4250(9)	107.832(2)	90
β/°	111.190(10)	99.0630(4)	82.9660(11)	99.2540(10)	77.8980(8)	77.8690(5)	77.4640(8)	103.059(2)	90.3160(10)
γ/°	90	90	87.5270(14)	90	75.6470(9)	81.8480(6)	89.6770(13)	94.394(2)	90
U/Å^3	1764.1(5)	1638.06(3)	1849.16(8)	1689.70(4)	1203.06(3)	3265.89(7)	1260.97(4)	1184.34(7)	4300.64(11)
Z	4	4	4	4	2	6	2	2	4
d_{calc}/g cm^{-3}	1.806	1.855	1.683	1.756	1.659	1.766	1.656	1.702	1.600
μ/mm^{-1}	1.450	1.559	1.166	1.274	0.979	1.081	0.938	0.998	0.684
Crystal size/mm	0.25 × 0.25 × 0.25	0.30 × 0.30 × 0.30	0.15 × 0.10 × 0.10	0.40 × 0.33 × 0.18	0.20 × 0.15 × 0.08	0.25 × 0.20 × 0.20	0.15 × 0.08 × 0.05	0.05 × 0.05 × 0.03	0.20 × 0.20 × 0.10
Reflections collected	3359	33639	21848	29040	22342	29069	20472	15723	41124
Independent reflections	3104	4771	8370	3794	5517	9023	4408	4172	7567
R(int)	0.0272	0.0334	0.0682	0.0323	0.0511	0.0684	0.0529	0.0893	0.0510
$R1$, w$R2$ [$I > 2\sigma(I)$]	0.0236, 0.0626	0.0222, 0.0531	0.0404, 0.0959	0.0217, 0.0608	0.0308, 0.0767	0.0384, 0.1024	0.0348, 0.0969	0.0497, 0.0902	0.0462, 0.1159
R indices (all data)	0.0262, 0.0654	0.0233, 0.0537	0.0526, 0.1033	0.0225, 0.0615	0.0379, 0.0808	0.0461, 0.1102	0.0434, 0.1052	0.0934, 0.1038	0.0520, 0.1190

As stated earlier, the asymmetric units in compounds **3a** and **7b**, were seen to contain, respectively, 2 and 3 molecules, while that in **10** comprises one cation, two triflate anions (one severely disordered) and 1.5 water molecules. The disordered triflate region of the electron density map was somewhat of a minefield, but optimal convergence was ultimately achieved by modelling the anion over two sites in a 60:40 ratio. One of phenyl rings in the cation also exhibited positional disorder in site-occupancy proportions of 55:35. The ADPs associated with the carbons in this disordered phenyl group were restrained to have similar values in the final convergence cycles. Hydrogen atoms in the full water molecule (based on O7) present in the motif of compound **10** were readily located and refined subject to distance restraints (0.89 Å from the parent atom and 1.45 Å from each other). Unfortunately, the hydrogen atoms associated with the half occupancy water (O8) could not be located and hence were omitted from the least-squares refinement.

CCDC reference numbers 217632–217640.

See http://www.rsc.org/suppdata/dt/b3/b309882f/ for crystallographic data in CIF or other electronic format.

Acknowledgements

The EPSRC is thanked for financial support and Johnson-Matthey is thanked for a generous loan of platinum metals.

References

1 E. K. van den Beuken, W. J. J. Smeets, A. L. Spek and B. L. Feringa, *Chem. Commun.*, 1998, 223.
2 E. Shirakawa and T. Hiyama, *J. Organomet. Chem.*, 1999, **576**, 169.
3 K. R. Reddy, K. Surekha, G.-H. Lee, S.-M. Peng and S.-T. Liu, *Organometallics*, 2000, **19**, 2637.
4 K. G. Moloy and J. L. Petersen, *J. Am. Chem. Soc.*, 1995, **117**, 7696.
5 C. D. Andrews, A. D. Burrows, J. M. Lynam, M. F. Mahon and M. T. Palmer, *New J. Chem.*, 2001, **25**, 824.
6 A. D. Burrows, M. F. Mahon, M. T. Palmer and M. Varrone, *Inorg. Chem.*, 2002, **41**, 1695.
7 H. Brunner and H. Weber, *Chem. Ber.*, 1985, **118**, 3380.
8 H. Brunner, W. Li and H. Weber, *J. Organomet. Chem.*, 1985, **288**, 359.
9 P. G. Cozzi, N. Zimmermann, R. Hilgraf, S. Schaffner and A. Pfaltz, *Adv. Synth. Catal.*, 2001, **343**, 450.
10 A. D. Burrows, M. F. Mahon and M. Varrone, *Inorg. Chim. Acta*, 2003, **350**, 152.
11 A. D. Burrows, *CrystEngComm*, 2001, **3**, 217.
12 A. D. Burrows, R. W. Harrington, M. F. Mahon, M. T. Palmer, F. Senia and M. Varrone, *Dalton Trans.*, 2003, 3717.
13 S. Fischer, L. K. Peterson and J. F. Nixon, *Can. J. Chem.*, 1974, **52**, 3981.
14 A. Frenzel, M. Gluth, R. Herbst-Irmer and U. Klingebiel, *J. Organomet. Chem.*, 1996, **514**, 281.
15 R. Jackstell, H. Klein, M. Beller, K.-D. Wiese and D. Röttger, *Eur. J. Org. Chem.*, 2001, 3871.
16 A. D. Burrows, M. F. Mahon and M. Varrone, unpublished results.
17 P. S. Pregosin and R. W. Kunz, ^{31}P and ^{13}C NMR of Transition Metal Phosphine Complexes, Springer-Verlag, 1979.
18 S. M. Aucott, A. M. Z. Slawin and J. D. Woollins, *J. Chem. Soc., Dalton Trans.*, 2000, 2559.
19 K. R. Reddy, W.-W. Tsai, K. Surekha, G.-H. Lee, S.-M. Peng, J.-T. Chen and S.-T. Liu, *J. Chem. Soc., Dalton Trans.*, 2002, 1776.
20 R. G. Pearson, *Inorg. Chem.*, 1973, **12**, 712.
21 G. P. C. M. Dekker, C. J. Elsevier, K. Vrieze and P. W. N. M. van Leeuwen, *Organometallics*, 1992, **11**, 1598; Y. Kayaki, H. Tsukamoto, M. Kaneko, I. Shimizu, A. Yamamoto, M. Tachikawa and T. Nakajima, *J. Organomet. Chem.*, 2001, **622**, 199.
22 G. A. Luinstra and P. H. P. Brinkmann, *Organometallics*, 1998, **17**, 5160; P. H. P. Brinkmann and G. A. Luinstra, *J. Organomet. Chem.*, 1999, **572**, 193.
23 E. Drent and P. H. M. Budzelaar, *Chem. Rev.*, 1996, **96**, 663.
24 K. R. Reddy, K. Surekha, G.-H. Lee, S.-M. Peng, J.-T. Chen and S.-T. Liu, *Organometallics*, 2001, **20**, 1292.
25 A. Sen, *Acc. Chem. Res.*, 1993, **26**, 303.
26 C. Bianchini, A. Meli, G. Müller, W. Oberhauser and E. Passaglia, *Organometallics*, 2002, **21**, 4965; C. S. Shultz, J. Ledford, J. M. DeSimone and M. Brookhart, *J. Am. Chem. Soc.*, 2000, **122**, 6351; F. C. Rix, M. Brookhart and P. S. White, *J. Am. Chem. Soc.*, 1996, **118**, 4746; J. Ledford, C. S. Shultz, D. P. Gates, P. S. White, J. M. DeSimone and M. Brookhart, *Organometallics*, 2001, **20**, 5266.
27 B. Milani, A. Scarel, G. Mestroni, S. Gladiali, R. Taras, C. Carfagna and L. Mosca, *Organometallics*, 2002, **21**, 1323; B. A. Markies, D. Kruis, M. H. P. Rietveld, K. A. N. Verkerk, J. Boersma, H. Kooijman, M. T. Lakin, A. L. Spek and G. Van Koten, *J. Am. Chem. Soc.*, 1995, **117**, 5263; S. Stoccoro, G. Minghetti, M. A. Cinellu, A. Zucca and M. Manassero, *Organometallics*, 2001, **20**, 4111.
28 G. P. C. M. Dekker, A. Buijs, C. J. Elsevier, K. Vrieze, P. W. N. M. van Leeuwen, W. J. J. Smeets, A. L. Spek, Y. F. Wang and C. H. Stam, *Organometallics*, 1992, **11**, 1937; K. R. Reddy, C.-L. Chen, Y.-H. Liu, S.-M. Peng, J.-T. Chen and S.-T. Liu, *Organometallics*, 1999, **18**, 2574; P. Braunstein, M. D. Fryzuk, M. Le Dall, F. Naud, S. J. Rettig and F. Speiser, *J. Chem. Soc., Dalton Trans.*, 2000, **7**, 1067; Y.-C. Chen, C.-L. Chen, J.-T. Chen and S.-T. Liu, *Organometallics*, 2001, **20**, 1285.
29 A. Sommazzi and F. Garbassi, *Prog. Polym. Sci.*, 1997, **22**, 1547.
30 H.-K. Luo and D.-G. Li, *J. Mol. Catal. A*, 2001, **171**, 23.
31 V. V. Grushin, *Chem. Rev.*, 1996, **96**, 2011; M. Portnoy and D. Milstein, *Organometallics*, 1994, **13**, 600.
32 I. Tóth and C. J. Elsevier, *Organometallics*, 1994, **13**, 2118.
33 M. Portnoy, F. Frolow and D. Milstein, *Organometallics*, 1991, **10**, 3960.
34 J. Chatt, L. M. Vallarino and L. M. Venanzi, *J. Chem. Soc.*, 1957, 3413.
35 D. Drew and J. R. Doyle, *Inorg. Synth.*, 1972, **13**, 47.
36 G. Giordano and R. H. Crabtree, *Inorg. Synth.*, 1990, **28**, 88.
37 R. E. Rülke, J. M. Ernsting, A. L. Spek, C. J. Elsevier, P. W. N. M. van Leeuwen and K. Vrieze, *Inorg. Chem.*, 1993, **32**, 5769.
38 A. D. Burrows, M. F. Mahon, S. P. Nolan and M. Varrone, *Inorg. Chem.*, 2003, **42**, 7227.